Exact two-component Hamiltonians for relativistic quantum chemistry: Two-electron picture-change corrections made simple

🆔 Stefan Knecht, 🆔 Michal Repisky, 🆔 Hans Jørgen Aagaard Jensen, et al.
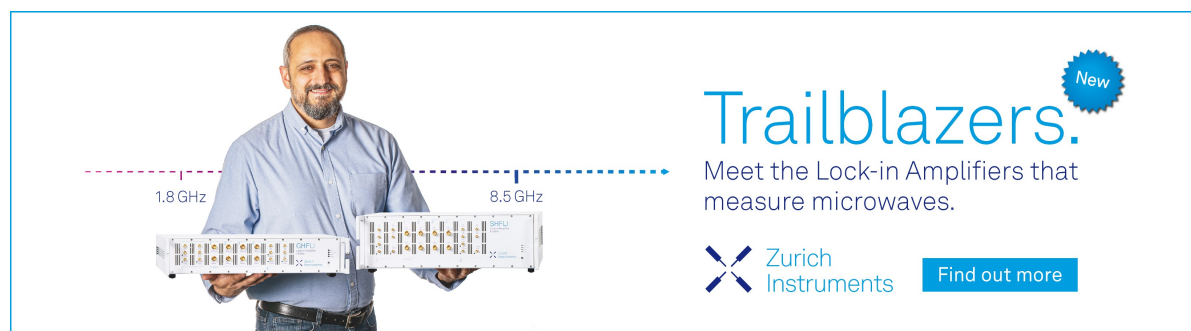
View Online   Export Citation   CrossMark

Exact two-component Hamiltonians for relativistic quantum chemistry: Two-electron picture-change corrections made simple

View Online   Export Citation   CrossMark

Stefan Knecht,[1,2,3,a] Michal Repisky,[4,b] Hans Jørgen Aagaard Jensen,[5] and Trond Saue[6]

AFFILIATIONS

[1] Algorithmiq Ltd, Kanavakatu 3C, FI-00160 Helsinki, Finland

[2] SHE Chemie, GSI Helmholtzzentrum für Schwerionenforschung GmbH, Planckstr. 1, 64291 Darmstadt, Germany

[3] Department of Chemistry, Johannes-Gutenberg Universität Mainz, Duesbergweg 10-14, 55128 Mainz, Germany

[4] Hylleraas Centre for Quantum Molecular Sciences, Department of Chemistry, UiT–The Arctic University of Norway, N-9037 Tromsø, Norway

[5] Department of Physics, Chemistry and Pharmacy, University of Southern Denmark, Campusvej 55, DK-5230 Odense M, Denmark

[6] Laboratoire de Chimie et Physique Quantiques (CNRS UMR 5626), Université Toulouse III – Paul Sabatier, 118 Route de Narbonne, F-31062 Toulouse Cedex, France

[a] Author to whom correspondence should be addressed: stefan@algorithmiq.fi
[b] Electronic mail: michal.repisky@uit.no

ABSTRACT

Based on self-consistent field (SCF) atomic mean-field (amf) quantities, we present two simple yet computationally efficient and numerically accurate matrix-algebraic approaches to correct both scalar-relativistic *and* spin–orbit two-electron picture-change effects (PCEs) arising within an exact two-component (X2C) Hamiltonian framework. Both approaches, dubbed amfX2C and e(xtended)amfX2C, allow us to uniquely tailor PCE corrections to mean-field models, viz. Hartree–Fock or Kohn–Sham DFT, in the latter case also avoiding the need for a point-wise calculation of exchange–correlation PCE corrections. We assess the numerical performance of these PCE correction models on spinor energies of group 18 (closed-shell) and group 16 (open-shell) diatomic molecules, achieving a consistent $\approx 10^{-5}$ Hartree accuracy compared to reference four-component data. Additional tests include SCF calculations of molecular properties such as absolute contact density and contact density shifts in copernicium fluoride compounds (CnF_n, n = 2,4,6), as well as equation-of-motion coupled-cluster calculations of x-ray core-ionization energies of 5d- and 6d-containing molecules, where we observe an excellent agreement with reference data. To conclude, we are confident that our (e)amfX2C PCE correction models constitute a fundamental milestone toward a universal and reliable relativistic two-component quantum-chemical approach, maintaining the accuracy of the parent four-component one at a fraction of its computational cost.

Published under an exclusive license by AIP Publishing. https://doi.org/10.1063/5.0095112

I. INTRODUCTION

Advancing with rapid strides in the past decades, relativistic quantum-chemical approaches are becoming a standard ingredient in the computational toolbox of theoretical chemists. Notwithstanding important steps forward to turn a fully relativistic quantum-chemical approach based on the four-component Dirac formalism into a handy tool,[1–9] much of the success is due to the

fast-paced development and implementation of efficient quasi-relativistic "exact" two-component approaches (X2C)[10] in various originally nonrelativistic popular quantum chemistry software packages within the past two decades. This has become possible by making use of a matrix-algebra formalism rather than setting out from an (order-by-order) operator-based formalism.[11–19]

In relativistic quantum chemistry, the common starting point for almost all of the matrix-algebra-based two-component (2c)

Hamiltonian approaches, whether formulated within an elimination *ansatz*[20–23] or in a unitary decoupling framework,[24–30] has been the four-component (4c) *one-electron* Dirac Hamiltonian in the electrostatic potential of fixed nuclei.[3] We will in the following refer to the 4c Hamiltonian used to construct a 2c model as the *defining* 4c Hamiltonian. In the case of the one-electron X2C Hamiltonian scheme (1eX2C), the two-electron (2e) interaction term is omitted from the defining 4c Dirac Hamiltonian. Consequently, the resulting 2c Hamiltonian is to be considered "exact" only with respect to the inclusion of 1e terms in the defining 4c Hamiltonian,[31] while the consideration of the 2e interaction is postponed till *after* having carried out the unitary decoupling of the 1e Hamiltonian and the ensuing restriction to the upper ("electrons-only") 2c spinor basis. Such an approach usually implies the use of the *untransformed* 2e interaction term in the 1eX2C basis set, giving rise to 2e picture-change effects (2ePCEs). A noticeable exception exists, though, and has been coined the molecular mean-field exact two-component approach (mmfX2C).[32] In contrast to the 1eX2C scheme, the mmfX2C *ansatz* is based on a unitary decoupling of the 4c molecular mean-field *Fock matrix* after having converged the 4c self-consistent field (SCF) Hartree–Fock equations. Although strictly matching with the SCF results of those obtained with the corresponding defining 4c Hamiltonian,[27,32] the mmfX2C approach will still be an approximation in any ensuing post-SCF electron correlation step for which the untransformed 2e interaction term replaces its complete (transformed) counterpart.

Hence, the extent to which 2ePCEs are accounted for in an X2C Hamiltonian based relativistic quantum-chemical framework is essential for its applicability to address the electronic structure theory problem in many-electron (molecular) systems involving elements across the entire Periodic Table.[31] To this end, we note that the 2e interaction term can be decomposed into a spinfree or scalar-relativistic (SC) as well as a spin-dependent or spin–orbit (SO) part,[1,33] where both the two-electron scalar-relativistic (2eSC) and two-electron spin–orbit (2eSO) terms serve as a screening of their 1e counterparts. Whereas much attention has been paid in the past to efficiently take into account 2eSO PCEs based on a variety of *ansätze*, the 2eSC contributions are curiously, less commonly included in correction schemes for 2ePCEs as has been comprehensively summarized in the Introduction of Ref. 34. Examples of approximate 2eSO corrections range from using (i) a parameterized model approach based on nuclear charges multiplied with element and angular-momentum specific screening factors in the evaluation of 1eSO integrals;[35,36] (ii) a mean-field SO approach,[37] which has been the basis for the widely popular AMFI module[38] interfaced, for example, with the software packages DIRAC,[5] OPENMOLCAS,[39] and DALTON;[40] (iii) an approach that exploits atomic model densities obtained within the framework of Kohn–Sham DFT (KS-DFT).[41–43] Interestingly, although the latter model-density-based correction schemes are rare examples that, in addition to corrections for 2eSO PCEs, do provide corrections for 2eSC PCEs, the resulting correction terms do not discriminate between the use of different exchange–correlation functionals employed in a *molecular* X2C Hamiltonian-based Kohn–Sham DFT calculation. The screening factors of type (i) are sometimes referred to as "Boettger factors" or as the screened–nuclear–spin–orbit (SNSO) approach.[44] In current usage, they have been obtained for a second-order, truncated 2c Hamiltonian *ansatz* (i.e., second-order Douglas–Kroll–Hess

(DKH2)) within the framework of density functional theory (DFT)[44] but are remarkably, also, commonly employed in X2C Hamiltonian-based wave function theory (WFT) approaches.[45–47] To overcome this discrepancy for their use in exact two-component theories, the original SNSO approach has been reparametrized based on atomic four-component Dirac–Hartree–Fock results.[48] The resulting *modified* SNSO approach led to further improvement for the calculation of molecular properties in a two-component framework with respect to the parent four-component results.[48,49]

In their most recent work on suitable 2ePCE corrections for the X2C Hamiltonian, Liu and Cheng[34] proposed an atomic mean-field (amf) approach that exploits a mean-field approximation for PCEs originating from the 2eSO contribution, dubbed SOX2CAMF by them, and combines "the four main ideas in relativistic quantum chemistry (. . .): the X2C decoupling scheme, the 1e approximation for SC effects (i.e., the neglect of the scalar 2e picture-change effects), the mean-field SO approach, and the atomic approximation for the 2eSO interactions."[34] Thus, a key feature of the SOX2CAMF model is that it does not require the evaluation of any *molecular* relativistic 2e integral. Although it has in the meantime been employed successfully in highly sophisticated electron correlation calculations of heavy-element complexes,[50] limitations of the underlying atomic approximation to account for 2eSO PCEs have recently been pointed out in the context of zero-field splittings of first row transition metal complexes.[51]

In this paper, we introduce an atomic mean-field (amfX2C) as well as an extended atomic mean-field (eamfX2C) approach within the X2C Hamiltonian framework that not only takes into account the above-mentioned four main ideas in relativistic quantum chemistry but also amends them such that the resulting amfX2C and eamfX2C approaches will bridge the gap between a full molecular 4c and mmfX2C framework in a computationally efficient, yet highly accurate, way. In contrast to most existing correction schemes for 2ePCE, our amfX2C and eamfX2C approaches are laid out to comprise *full* 2ePCE corrections, that is, to treat the 2eSO *and* 2eSC ones on the same footing, whether they arise from the (relativistic) 2e Coulomb, Coulomb–Gaunt, or Coulomb–Breit interaction. Moreover, our *ansatz* takes into account the characteristics of the underlying correlation framework, viz., WFT or (KS-)DFT, which enables us to introduce tailor-made exchange–correlation-specific corrections for 2ePCEs. Setting out from the idea of an amf approach within the amfX2C Hamiltonian model—formulated for a WFT-based HF and a DFT framework in Secs. II A and II B, respectively—the *extended* amfX2C approach encompasses two-center 2e contributions obtained in a molecular framework. The implications arising from the resulting eamfX2C approach, including its potential shortcomings and particular advantages, are then discussed in Sec. II C. The numerical accuracy of both (e)amfX2C Hamiltonian models are assessed based on the calculation of a variety of valence and core-like molecular properties in Sec. IV where the computational details are given in Sec. III. We summarize our results and findings in Sec. V and summarize prospects for future developments.

II. THEORY

A. The amfX2C Hamiltonian–Hartree–Fock framework

A convenient starting point for our derivations to arrive at suitable corrections for 2ePCEs in an X2C Hamiltonian

framework is to consider the closed-shell 4c HF equations based on the Dirac–Coulomb Hamiltonian,

$$\boldsymbol{F}^{4c}\boldsymbol{c}_i^{4c} = \boldsymbol{c}_i^{4c}\epsilon_i^{4c}. \tag{1}$$

For convenience (see below), we express these equations in the orthonormal basis obtained from the initial atomic orbital (AO)-basis by some suitable orthogonalization procedure.[52] The HF energy and the Fock matrix have their usual definitions,

$$E^{4c} = E^{4c,1e} + E^{4c,2e} = \sum_{\mu\nu} h_{\mu\nu}^{4c} D_{\nu\mu}^{4c} + \frac{1}{2}\sum_{\mu\nu\kappa\lambda} D_{\nu\mu}^{4c} G_{\mu\nu,\kappa\lambda}^{4c} D_{\lambda\kappa}^{4c}, \tag{2}$$

$$F_{\mu\nu}^{4c} = F_{\mu\nu}^{4c,1e} + F_{\mu\nu}^{4c,2e} = h_{\mu\nu}^{4c} + \sum_{\kappa\lambda} G_{\mu\nu,\kappa\lambda}^{4c} D_{\lambda\kappa}^{4c} = \frac{dE^{4c}}{dD_{\nu\mu}^{4c}}, \tag{3}$$

in terms of the atomic orbital (AO) density matrix given by

$$D_{\mu\nu}^{4c} = \sum_i^{occ} c_{\mu i}^{4c} c_{\nu i}^{4c*} \tag{4}$$

and the matrix of anti-symmetrized two-electron AO integrals given by

$$G_{\mu\nu,\kappa\lambda}^{4c} = \mathcal{I}_{\mu\nu,\kappa\lambda}^{4c} - \mathcal{I}_{\mu\lambda,\kappa\nu}^{4c};$$
$$\mathcal{I}_{\mu\nu,\kappa\lambda}^{4c} \equiv \iint \Omega_{\mu\nu}^{4c}(\boldsymbol{r}_1) r_{12}^{-1} \Omega_{\kappa\lambda}^{4c}(\boldsymbol{r}_2) d^3\boldsymbol{r}_1 d^3\boldsymbol{r}_2, \tag{5}$$

the latter expressed in terms of overlap distribution functions,[6]

$$\Omega_{\mu\nu}^{4c}(\boldsymbol{r}) \equiv \int \chi_\mu^\dagger(\boldsymbol{r}') \delta^3(\boldsymbol{r}'-\boldsymbol{r})\chi_\nu(\boldsymbol{r}') d^3\boldsymbol{r}' = \chi_\mu^\dagger(\boldsymbol{r})\chi_\nu(\boldsymbol{r}), \tag{6}$$

over two-component basis functions $\chi_\mu(\boldsymbol{r})$; formally, the basis functions are four-component objects, but with the lower or upper two components zero according to whether they are large (L) or small (S).

The *converged* HF equations, Eq. (1), form the starting point for the mmfX2C approach,[32] where the Fock matrix and corresponding positive-energy molecular-orbital (MO) coefficients (+) are picture-changed to 2c form. Our computer implementations[28,30] generate the picture-change transformation matrix $\boldsymbol{U}$ in orthonormal basis since this provides control on possible linear dependencies and simplifies the construction of the appropriate metric.[29] The picture-change matrix is subsequently transformed back to the initial AO-basis. For simplicity, and without loss of generality, we shall consider the PC-transformation in orthonormal basis. Starting from Eq. (1), we, therefore, write

$$\tilde{F}_{\mu\nu}^{2c} \equiv \left[\boldsymbol{U}^\dagger \boldsymbol{F}^{4c}\boldsymbol{U}\right]_{\mu\nu}^{LL}; \quad \tilde{c}_{\mu i}^{2c} \equiv \left[\boldsymbol{U}^\dagger \boldsymbol{c}^{4c}\right]_{\mu i}^{L+} \tag{7}$$

(note that we use tildes to indicate picture-change transformed quantities). These quantities, together with the anti-symmetrized two-electron AO integrals, Eq. (5), are then used to build the normal-ordered Hamiltonian for use in subsequent wave function-based correlation methods.

In the present case, we rather seek to carry out the SCF-iterations themselves in 2c mode but in a manner such that we optimally reproduce the 4c results. A first important observation comes from consideration of the picture-change transformed Fock matrix given by

$$\tilde{F}_{\mu\nu}^{2c} = \sum_{XY}\sum_{\alpha\beta}\left[U^\dagger\right]_{\mu\alpha}^{LX}\left[F^{4c}\right]_{\alpha\beta}^{XY}\left[U\right]_{\beta\nu}^{YL}; \quad X,Y \in L, S. \tag{8}$$

Noting that the positive-energy 4c MO-coefficients can be expressed in terms of their 2c counterparts,

$$\boldsymbol{c}^{4c;+} = \boldsymbol{U}\tilde{\boldsymbol{c}}^{2c} \Rightarrow \left[c^{4c}\right]_{\mu i}^{X+} = \sum_\nu \left[U\right]_{\mu\nu}^{XL}\left[\tilde{c}^{2c}\right]_{\nu i}; \quad X \in L, S, \tag{9}$$

we can reformulate the two-electron 2c Fock matrix as

$$\tilde{F}_{\mu\nu}^{2c,2e} = \sum_{XY}\sum_{\alpha\beta}\left[U^\dagger\right]_{\mu\alpha}^{LX}\left[F^{4c,2e}\right]_{\alpha\beta}^{XY}\left[U\right]_{\beta\nu}^{YL}$$

$$= \sum_{XY}\sum_{\alpha\beta}\left[U^\dagger\right]_{\mu\alpha}^{LX}\left\{\sum_{UV}\sum_{\gamma\delta}\left[G^{4c}\right]_{\alpha\beta,\gamma\delta}^{XY,UV}\left[D^{4c}\right]_{\delta\gamma}^{VU}\right\}\left[U\right]_{\beta\nu}^{YL}$$

$$= \sum_{XY}\sum_{\alpha\beta}\left[U^\dagger\right]_{\mu\alpha}^{LX}\left\{\sum_{UV}\sum_{\gamma\delta}\left[G^{4c}\right]_{\alpha\beta,\gamma\delta}^{XY,UV}\sum_{\kappa\lambda}\right.$$
$$\left. \times \sum_i \left[U\right]_{\delta\kappa}^{VL}\left[\tilde{c}^{2c}\right]_{\kappa i}\left[\tilde{c}^{2c*}\right]_{\lambda i}\left[U^*\right]_{\gamma\lambda}^{UL}\right\}\left[U\right]_{\beta\nu}^{YL} \tag{10}$$

$$= \sum_{\kappa\lambda}\left\{\sum_{XYUV}\sum_{\alpha\beta\gamma\delta}\left[U^\dagger\right]_{\mu\alpha}^{LX}\left[U^\dagger\right]_{\lambda\gamma}^{LU}\left[G^{4c}\right]_{\alpha\beta,\gamma\delta}^{XY,UV}\left[U\right]_{\delta\kappa}^{VL}\left[U\right]_{\beta\nu}^{YL}\right\}$$
$$\times \left[\tilde{D}^{2c}\right]_{\kappa\lambda}; \quad X,Y,U,V \in L, S. \tag{11}$$

As a consequence,

$$\tilde{F}_{\mu\nu}^{2c} = \tilde{h}_{\mu\nu}^{2c} + \sum_{\kappa\lambda}\tilde{G}_{\mu\nu,\kappa\lambda}^{2c}\tilde{D}_{\lambda\kappa}^{2c}. \tag{12}$$

We see that the picture-change transformed Fock matrix can be expressed in terms of the picture-changed transformed coefficients as well as the picture-changed one- and two-electron integrals. By similar manipulations, we can also show that the 4c HF energy can be expressed in terms of corresponding 2c quantities, that is,

$$E^{4c} = \sum_{XY}\sum_{\mu\nu}\left[h^{4c}\right]_{\mu\nu}^{XY}\left[D^{4c}\right]_{\nu\mu}^{YX} + \frac{1}{2}\sum_{XYUV}$$

$$\times \sum_{\mu\nu\kappa\lambda}\left[D^{4c}\right]_{\nu\mu}^{YX}\left[G^{4c}\right]_{\mu\nu,\kappa\lambda}^{XYUV}\left[D^{4c}\right]_{\lambda\kappa}^{VU}$$

$$= \sum_{\mu\nu}\left[\tilde{h}^{2c}\right]_{\mu\nu}\left[\tilde{D}^{2c}\right]_{\nu\mu} + \frac{1}{2}\sum_{\mu\nu\kappa\lambda}\left[\tilde{D}^{2c}\right]_{\nu\mu}\left[\tilde{G}^{2c}\right]_{\mu\nu,\kappa\lambda}$$

$$\times \left[\tilde{D}^{2c}\right]_{\lambda\kappa} = \tilde{E}^{2c,1e} + \tilde{E}^{2c,2e}. \tag{13}$$

We conclude that provided we start from the *correctly transformed* set of integrals, the 2c SCF will converge to the coefficients $\{\tilde{c}_i^{2c}\}$ corresponding to the converged 4c SCF and we shall furthermore

reproduce the positive orbital energies as well as total energy of the parent 4c HF. However, the picture-change transformation $\boldsymbol{U}$ associated with the converged 4c Fock matrix is *not* available at the start of the SCF-iterations, forcing us to introduce approximations.

With this in view, a second important observation arises from comparison of Eq. (12) with the Fock matrix built with *untransformed* two-electron integrals $G^{2c}_{\mu\nu,\kappa\lambda}$,

$$F^{2c}_{\mu\nu} = \tilde{h}^{2c}_{\mu\nu} + \sum_{\kappa\lambda} G^{2c}_{\mu\nu,\kappa\lambda} \tilde{D}^{2c}_{\lambda\kappa}. \quad (14)$$

We immediately find that their difference expresses the picture-change correction of the two-electron integrals,

$$\Delta\tilde{F}^{2c}_{\mu\nu} = \tilde{F}^{2c}_{\mu\nu} - F^{2c}_{\mu\nu} = \sum_{\kappa\lambda} \Delta\tilde{G}^{2c}_{\mu\nu,\kappa\lambda} \tilde{D}^{2c}_{\lambda\kappa};$$
$$\Delta\tilde{G}^{2c}_{\mu\nu,\kappa\lambda} = \tilde{G}^{2c}_{\mu\nu,\kappa\lambda} - G^{2c}_{\mu\nu,\kappa\lambda}. \quad (15)$$

Moreover, this differential Fock matrix may be used to correct the two-electron HF energy,

$$\tilde{E}^{2c,2e} = \frac{1}{2}\sum_{\mu\nu\kappa\lambda}\tilde{D}^{2c}_{\nu\mu}\tilde{G}^{2c}_{\mu\nu,\kappa\lambda}\tilde{D}^{2c}_{\lambda\kappa} = \frac{1}{2}\sum_{\mu\nu}\tilde{D}^{2c}_{\nu\mu}$$
$$\times \underbrace{\sum_{\kappa\lambda} G^{2c}_{\mu\nu,\kappa\lambda}\tilde{D}^{2c}_{\lambda\kappa}}_{F^{2c,2e}_{\mu\nu}} + \frac{1}{2}\sum_{\mu\nu}\tilde{D}^{2c}_{\nu\mu}\underbrace{\sum_{\kappa\lambda}\Delta\tilde{G}^{2c}_{\mu\nu,\kappa\lambda}\tilde{D}^{2c}_{\lambda\kappa}}_{\Delta\tilde{F}^{2c,2e}_{\mu\nu}}. \quad (16)$$

We now seek a suitable approximation for the differential two-electron Fock matrix $\Delta\tilde{F}^{2c,2e}$. In line with previous authors, we exploit the expected local atomic nature of the two-electron picture-change corrections, but we will impose the condition that the scheme should reproduce *atomic* 4c SCF calculations *exactly* at the 2c level. We accordingly start from a superposition of converged atomic quantities rather than the converged molecular one, i.e.,

$$\Delta\tilde{F}^{2c,2e} \simeq \Delta\tilde{F}^{2c,2e}_{\oplus} = \bigoplus_{K=1}^{M} \Delta\tilde{F}^{2c}_{K}[\tilde{D}^{2c}_{K}], \quad (17)$$

where K runs over all atoms in an M-atomic system. Such an approach defines our *atomic mean-field exact two-component* scheme, denoted as amfX2C. We emphasize that the picture-change correction given by Eq. (17) should be expressed in the original AO-basis rather than the orthonormal one in order to avoid mixing of basis functions from different centers. However, in order to avoid notational overload, we do not distinguish matrix quantities in the two different bases.

Due to the atomic nature of amfX2C two-electron picture-change corrections, their evaluation scales linearly with the system size (or sub-linearly if there are multiple instances of an atomic type). To summarize the essentials, we propose the following computational scheme to arrive at the amfX2C model:

1. For each atomic type K, we perform a 4c Kramers-restricted (KR) average-of-configuration (AOC) HF calculation[53] — or, if the latter is not available, a 4c KR fractional occupation HF calculation.
2. The converged atomic Fock matrix $\boldsymbol{F}^{4c}_{K}$ is exactly block-diagonalized to give its 2c counterpart $\tilde{\boldsymbol{F}}^{2c}_{K}$ as well as picture-changed coefficients $\tilde{\boldsymbol{c}}^{2c}_{K}$ and density matrix $\tilde{\boldsymbol{D}}^{2c}_{K}$.

3. Using the latter quantity, we build the atomic 2c Fock matrix $\boldsymbol{F}^{2c}_{K}[\tilde{\boldsymbol{D}}^{2c}_{K}]$ with untransformed two-electron integrals, Eq. (14).
4. The differential atomic Fock matrix $\Delta\tilde{\boldsymbol{F}}^{2c}_{K}[\tilde{\boldsymbol{D}}^{2c}_{K}]$ is now built according to Eq. (15).
5. The atomic matrices $\Delta\tilde{\boldsymbol{F}}^{2c}_{K}$ and $\boldsymbol{F}^{4c,2e}_{K}$ are then inserted in the appropriate atomic blocks to form approximate molecular two-electron picture-change correction matrix $(\Delta\tilde{\boldsymbol{F}}^{2c,2e}_{\oplus})$, Eq. (17), and approximate molecular two-electron Fock matrix $(\boldsymbol{F}^{4c,2e}_{\oplus})$, respectively,

$$\boldsymbol{F}^{4c,2e} \simeq \boldsymbol{F}^{4c,2e}_{\oplus} = \bigoplus_{K=1}^{M} \boldsymbol{F}^{4c,2e}_{K}[\boldsymbol{D}^{4c}_{K}]. \quad (18)$$

6. The molecular X2C decoupling matrix $\boldsymbol{U}$ is built from $\boldsymbol{h}^{4c} + \boldsymbol{F}^{4c,2e}_{\oplus}$.
7. Finally, SCF-iterations are carried out with amfX2C expressions that approximate the exact molecular Fock matrix and energy expressions,

$$\tilde{F}^{2c}_{\mu\nu} \simeq \tilde{F}^{\mathrm{amfX2C}}_{\mu\nu} = \underbrace{\tilde{h}^{2c}_{\mu\nu} + \Delta\tilde{F}^{2c,2e}_{\oplus,\mu\nu}}_{\text{static term}} + \underbrace{F^{2c,2e}_{\mu\nu}[\tilde{\boldsymbol{D}}^{2c}]}_{\text{dynamic term}}, \quad (19)$$

$$\tilde{E}^{2c} \simeq \tilde{E}^{\mathrm{amfX2C}} = \sum_{\mu\nu}\tilde{D}^{2c}_{\nu\mu}\left(\tilde{h}^{2c}_{\mu\nu} + \frac{1}{2}\Delta\tilde{F}^{2c,2e}_{\oplus,\mu\nu} + \frac{1}{2}F^{2c,2e}_{\mu\nu}[\tilde{\boldsymbol{D}}^{2c}]\right). \quad (20)$$

A pseudo-code describing the essential steps of our amfX2C approach for both HF and Kohn–Sham DFT theory is listed in Algorithm 1.

B. The amfX2C Hamiltonian–Kohn–Sham DFT framework

Section II A has so far exclusively focused on a discussion of 2ePCE corrections within a mean-field HF scheme. As indicated in Algorithm 1, the proposed amfX2C scheme has also the appealing feature that it can straightforwardly be extended to a KS-DFT framework.

1. The closed-shell case

We first consider the closed-shell molecular case and again start from Eq. (1), but with the Fock matrix replaced by the KS one. The 4c energy and KS matrix read

$$E^{4c} = \sum_{\mu\nu}h^{4c}_{\mu\nu}D^{4c}_{\nu\mu} + \frac{1}{2}\sum_{\mu\nu\kappa\lambda}D^{4c}_{\nu\mu}G^{\omega;4c}_{\mu\nu,\kappa\lambda}D^{4c}_{\lambda\kappa} + E^{4c}_{xc}[n^{4c}], \quad (21)$$

$$F^{4c}_{\mu\nu} = h^{4c}_{\mu\nu} + \sum_{\kappa\lambda}G^{\omega;4c}_{\mu\nu,\kappa\lambda}D^{4c}_{\lambda\kappa} + \int v_{xc}[n^{4c}](\boldsymbol{r})\Omega^{4c}_{\mu\nu}(\boldsymbol{r})d^3\boldsymbol{r};$$
$$v_{xc}[n](\boldsymbol{r}) = \frac{\delta E_{xc}}{\delta n(\boldsymbol{r})}. \quad (22)$$

Here, we have generalized the anti-symmetrized two-electron AO integrals of Eq. (5) to include the weight ω of exact exchange. As

Algorithm 1. Pseudo-code highlighting the essential steps for the amfX2C approach.

1: /* Initialize the molecular two-electron (2e) Fock matrices and XC energy */
2: $\boldsymbol{F}_{\oplus}^{4c,2e} = \boldsymbol{0}$; $\Delta\tilde{\boldsymbol{F}}_{\oplus}^{2c,2e} = \boldsymbol{0}$; $\Delta\tilde{E}_{xc,\oplus}^{2c} = 0$
3: **for all** `unique atom types` K $\in$`molecule` **do**
4:   Let $\{\mu,\nu\} \in$ atomic basis K
5:   /* Solve the 4c SCF equation */
6:   $\boldsymbol{F}_K^{4c}\boldsymbol{c}_K^{4c} = \boldsymbol{c}_K^{4c}\boldsymbol{\epsilon}_K^{4c}$ with $F_{K,\mu\nu}^{4c} = \begin{cases} F_{K,\mu\nu}^{4c,\text{HF}}[\boldsymbol{D}_K^{4c}] = h_{K,\mu\nu}^{4c} + \sum\limits_{\gamma,\delta\in K} G_{\mu\nu,\gamma\delta}^{4c} D_{K,\delta\gamma}^{4c} \\ F_{K,\mu\nu}^{4c,\text{KS}}[\boldsymbol{D}_K^{4c}] = h_{K,\mu\nu}^{4c} + \sum\limits_{\gamma,\delta\in K} G_{\mu\nu,\gamma\delta}^{\omega,4c} D_{K,\delta\gamma}^{4c} + F_{K,\mu\nu}^{4c,\text{xc}}[\boldsymbol{D}_K^{4c}] \end{cases}$
7:   /* Add K-th atomic 2e Fock contrib. $\boldsymbol{F}_K^{4c,2e}$ to the corresponding molecular block */
8:   $\boldsymbol{F}_{\oplus}^{4c,2e} \leftarrow \boldsymbol{F}_K^{4c,2e}$ with $F_{K,\mu\nu}^{4c,2e} = \begin{cases} F_{K,\mu\nu}^{4c,\text{HF}}[\boldsymbol{D}^{4c_K}] - h_{K,\mu\nu}^{4c} \\ F_{K,\mu\nu}^{4c,\text{KS}}[\boldsymbol{D}_K^{4c}] - h_{K,\mu\nu}^{4c} \end{cases}$
9:   /* Evaluate the atomic X2C decoupling matrix $\boldsymbol{U}_K$ from $\boldsymbol{F}_K^{4c}$ and calculate */
10:   $\tilde{\boldsymbol{D}}_K^{2c} = \left[\boldsymbol{U}_K^\dagger \boldsymbol{D}_K^{4c} \boldsymbol{U}_K\right]^{\text{LL}}$; $\Delta\tilde{\boldsymbol{F}}_K^{2c,2e} = \left[\boldsymbol{U}_K^\dagger \boldsymbol{F}_K^{4c,2e} \boldsymbol{U}_K\right]^{\text{LL}} - \boldsymbol{F}_K^{2c,2e}$
11:   /* where the latter term facilitates untransformed quantities G^{2c}, $G^{\omega,2c}$, and $F_K^{2c,\text{xc}}$ */
12:   $F_{K,\mu\nu}^{2c,2e} = \begin{cases} F_{K,\mu\nu}^{2c,2e,\text{HF}}[\tilde{\boldsymbol{D}}_K^{2c}] = \sum\limits_{\gamma,\delta\in K} G_{\mu\nu,\gamma\delta}^{2c} \tilde{D}_{K,\delta\gamma}^{2c} \\ F_{K,\mu\nu}^{2c,2e,\text{KS}}[\tilde{\boldsymbol{D}}_K^{2c}] = \sum\limits_{\gamma,\delta\in K} G_{\mu\nu,\gamma\delta}^{\omega,2c} \tilde{D}_{K,\delta\gamma}^{2c} + F_{K,\mu\nu}^{2c,\text{xc}}[\tilde{\boldsymbol{D}}_K^{2c}] \end{cases}$
13:   /* Add K-th atomic block of the picture-change error correction to the corresponding molecular block. In case of DFT, add also the atomic XC energy correction: */
14:   $\Delta\tilde{\boldsymbol{F}}_{\oplus}^{2c,2e} \leftarrow \Delta\tilde{\boldsymbol{F}}_K^{2c,2e}$; $\Delta\tilde{E}_{xc,\oplus}^{2c} \leftarrow \left(E_{xc,K}^{4c}[\boldsymbol{D}_K^{4c}] - E_{xc,K}^{2c}[\tilde{\boldsymbol{D}}_K^{2c}]\right)$
15: **end for**
16: Let $\{\mu,\nu\} \in$ full molecular basis
17: /* Evaluate the molecular X2C decoupling matrix $\boldsymbol{U}$ from */
18: $\tilde{\boldsymbol{h}}^{4c} = \boldsymbol{h}^{4c} + \boldsymbol{F}_{\oplus}^{4c,2e}$
19: /* Solve the 2c SCF equation with the amfX2C Fock matrix operator */
20: $\boldsymbol{F}^{2c}\boldsymbol{c}^{2c} = \boldsymbol{c}^{2c}\boldsymbol{\epsilon}^{2c}$ with $F_{\mu\nu}^{2c} \equiv F_{\mu\nu}^{\text{amfX2C}} = \underbrace{\left[\boldsymbol{U}^\dagger \boldsymbol{h}^{4c} \boldsymbol{U}\right]_{\mu\nu}^{\text{LL}} + \Delta\tilde{F}_{\oplus,\mu\nu}^{2c,2e}}_{\text{static terms}} + \underbrace{F_{\mu\nu}^{2c,2e}[\boldsymbol{D}^{2c}]}_{\text{dynamic term}}$

---

usual, E_{xc} and v_{xc} refer to the exchange–correlation (xc) energy functional and the corresponding potential, respectively.

Formally, E_{xc} may be expressed as an integral over an xc energy density ε_{xc},

$$E_{xc}[n] = \int \varepsilon_{xc}[n](\boldsymbol{r}) d^3\boldsymbol{r}, \qquad (23)$$

which is itself a functional of the number density (n). This allows, for instance, the electron number to be known locally such that the derivative discontinuity can be obeyed.[54] Crucial for the following, though, is that density functional approximations (DFA) employ *local ansätze*. For instance, on the second rung of the "Jacob's ladder" of DFA,[55,56] we find the generalized gradient approximation (GGA)

$$E_{xc}[n] = \int \varepsilon_{xc}^{\text{GGA}}(n(\boldsymbol{r}), g(\boldsymbol{r})) d^3\boldsymbol{r}; \quad g(\boldsymbol{r}) = \nabla n(\boldsymbol{r}) \cdot \nabla n(\boldsymbol{r}), \quad (24)$$

where each integration point just needs local input.

Proceeding at the GGA/hybrid level, we find that the picture-changed KS matrix can be expressed as

$$\tilde{F}_{\mu\nu}^{2c} = \tilde{h}_{\mu\nu}^{2c} + \sum_{\kappa\lambda} \tilde{G}_{\mu\nu,\kappa\lambda}^{\omega;2c} \tilde{D}_{\lambda\kappa}^{2c} + \int v_{xc}^{\text{GGA}}\left(n^{4c}(\boldsymbol{r}), g^{4c}(\boldsymbol{r})\right) \tilde{\Omega}_{\mu\nu}^{2c}(\boldsymbol{r}) d^3\boldsymbol{r}. \tag{25}$$

We again recover an expression in terms of picture-changed quantities, but the xc potential is seen to still use 4c variables as input. However, proceeding as in the HF case [cf. Eq. (13) in Sec. II A], the number density can be re-expressed in terms of 2c quantities,

$$n^{4c}(\boldsymbol{r}) = \sum_{XY}\sum_{\mu\nu} \left[\Omega^{4c}(\boldsymbol{r})\right]_{\mu\nu}^{XY}\left[D^{4c}\right]_{\nu\mu}^{YX}$$
$$= \sum_{\mu\nu} \left[\tilde{\Omega}^{2c}(\boldsymbol{r})\right]_{\mu\nu}\left[\tilde{D}^{2c}\right]_{\nu\mu} = \tilde{n}^{2c}(\boldsymbol{r}). \tag{26}$$

Since the (correctly!) picture-changed transformed 2c number density $\tilde{n}^{2c}$ is identical to the parent 4c quantity at all points in space, this equivalence will also hold for their gradients, which allows us to write

$$g^{4c}(\boldsymbol{r}) = \nabla\tilde{n}^{2c}(\boldsymbol{r}) \cdot \nabla\tilde{n}^{2c}(\boldsymbol{r}) = \tilde{g}^{2c}(\boldsymbol{r}). \tag{27}$$

This also means that the xc energy and potential can be expressed entirely in terms of 2c quantities

$$\tilde{E}_{xc}^{2c} = \int \varepsilon_{xc}^{GGA}\big(\tilde{n}^{2c}(\boldsymbol{r}), \tilde{g}^{2c}(\boldsymbol{r})\big)d^3\boldsymbol{r}, \tag{28}$$

$$\tilde{F}_{\mu\nu}^{2c,\,xc} = \int v_{xc}^{GGA}\big(\tilde{n}^{2c}(\boldsymbol{r}), \tilde{g}^{2c}(\boldsymbol{r})\big)\tilde{\Omega}_{\mu\nu}^{2c}(\boldsymbol{r})d^3\boldsymbol{r}. \tag{29}$$

In passing, we note that the direct use of the GGA xc potential leads to contributions of the form

$$F_{\mu\nu}^{xc} = \int v_{xc}^{GGA}(\boldsymbol{r})\Omega_{\mu\nu}(\boldsymbol{r})d^3\boldsymbol{r};$$

$$v_{xc}^{GGA}(\boldsymbol{r}) = \left[\frac{\partial \varepsilon_{xc}^{GGA}}{\partial n} - 2\nabla \cdot \left(\left(\frac{\partial \varepsilon_{xc}^{GGA}}{\partial g}\right)\nabla n\right)\right](\boldsymbol{r}). \tag{30}$$

However, the second term of the GGA potential will require the expensive calculation of the Hessian of the number density ($\nabla^2 n$), so usually a derivative is shifted over to the overlap distribution $\Omega_{\mu\nu}(\boldsymbol{r})$, using integration by parts, giving

$$F_{\mu\nu}^{xc} = \int \left[\frac{\partial \varepsilon_{xc}^{GGA}}{\partial n}\Omega_{\mu\nu}(\boldsymbol{r}) + 2\left(\frac{\partial \varepsilon_{xc}^{GGA}}{\partial g}\right)\nabla n \cdot \nabla \Omega_{\mu\nu}(\boldsymbol{r})\right]d^3\boldsymbol{r}. \tag{31}$$

Proceeding as above, the corresponding 2c quantity is found to be

$$\tilde{F}_{\mu\nu}^{2c,\,xc} = \int \left[\frac{d\varepsilon_{xc}^{GGA}}{dn}\tilde{\Omega}_{\mu\nu}^{2c}(\boldsymbol{r}) + 2\left(\frac{\partial \varepsilon_{xc}^{GGA}}{\partial g}\right)\nabla n^{4c} \cdot \nabla \tilde{\Omega}_{\mu\nu}^{2c}(\boldsymbol{r})\right]d^3\boldsymbol{r}. \tag{32}$$

Again using integration by parts, we may recover Eq. (29). These manipulations are thereby seen to commute with the picture-change transformation, albeit only in the exact case. For simplicity, we will continue with the form of Eq. (30).

Just as in the case of HF, we will argue that, if the 2c calculation is carried out with the correctly transformed overlap distribution $\tilde{\Omega}_{\mu\nu}^{2c}(\boldsymbol{r})$, in addition to the picture-changed one- and two-electron integrals, it will converge to the picture-changed coefficients $\tilde{c}^{2c}$ obtained from the corresponding 4c calculation. However, again the correct decoupling matrix $\boldsymbol{U}$, i.e., the one associated with the *converged* KS matrix, is not available at the start of calculations and so, we will have to seek approximations. One option, pursued by Iakabata and Nakai,[57] is to use the decoupling matrix $\boldsymbol{U}$ associated with the Dirac Hamiltonian instead. The point-wise picture-change transformation of the overlap distribution, even with local approximations, adds significant computational cost, though, and the chosen decoupling matrix $\boldsymbol{U}$ is not optimal. An alternative would be to make picture-change corrections to the number density, starting from

$$\Delta \tilde{n}^{2c}(\boldsymbol{r}) = \tilde{n}^{2c}(\boldsymbol{r}) - n^{2c}(\boldsymbol{r}) = n^{4c}(\boldsymbol{r}) - n^{2c}(\boldsymbol{r}). \tag{33}$$

Due to the local nature of the corrections, we would expect these corrections to be separable into atomic contributions, possibly approximated by model densities (see e.g., Refs. 41 and 42), that is

$$\Delta \tilde{n}^{2c}(\boldsymbol{r}) \simeq \sum_{K=1}^{M} \Delta \tilde{n}_K^{2c}(\boldsymbol{r}). \tag{34}$$

Here, it is important to stress that the atomic number density n_K^{2c} (without the tilde) is untransformed in the sense that it employs an *untransformed* overlap distribution matrix $\boldsymbol{\Omega}_K^{2c}$ but the *correctly transformed* coefficients $\{\tilde{c}_{K,i}^{2c}\}$ corresponding to the parent 4c atomic calculation. Since we expect $\Delta \tilde{n}_K^{2c}(\boldsymbol{r})$ to be nonzero only in the deep atomic core, one could exploit spherical symmetry by calculating the correction on a *radial* grid. However, we have not pursued this approach, since it still involves point-wise corrections, albeit over a significantly reduced number of integration points.

Instead, we propose the following scheme which integrates nicely with the scheme proposed for HF: For each atomic species K, we run a 4c KR fractional occupation KS-calculation that provides the converged atomic KS matrix F_K^{4c}. From it, we can directly extract the atomic decoupling matrix $\boldsymbol{U}_K$ and the corresponding picture-changed KS matrix $\tilde{F}_K^{2c}$, notably containing $\tilde{F}_K^{2c,\,xc}$. We next build the untransformed equivalent

$$F_{K;\mu\nu}^{2c,\,xc} = \int v_{xc}^{GGA}\big(n_K^{2c}(\boldsymbol{r}), g_K^{2c}(\boldsymbol{r})\big)\Omega_{K;\mu\nu}^{2c}(\boldsymbol{r})d^3\boldsymbol{r}, \tag{35}$$

using the correctly picture-changed transformed coefficients $\tilde{c}_K^{2c}$. Our amfX2C picture-change correction to the xc potential is then obtained from atomic quantities as

$$\Delta \tilde{F}^{2c,\,xc} \simeq \Delta \tilde{F}_{\oplus}^{2c,\,xc} = \bigoplus_{K=1}^{M} \Delta \tilde{F}_K^{2c,\,xc};$$

$$\Delta \tilde{F}_K^{2c,\,xc} = \tilde{F}_K^{2c,\,xc} - F_K^{2c,\,xc}. \tag{36}$$

Similarly, the xc energy is corrected by first writing $\tilde{E}_{xc}^{2c} = E_{xc}^{2c} + \Delta \tilde{E}_{xc}^{2c}$ and then seeking an atomic approximation to the correction

$$\Delta \tilde{E}_{xc}^{2c} = \int \varepsilon_{xc}^{GGA}\big(\tilde{n}^{2c}(\boldsymbol{r}), \tilde{g}^{2c}(\boldsymbol{r})\big)d^3\boldsymbol{r}$$

$$- \int \varepsilon_{xc}^{GGA}\big(n^{2c}(\boldsymbol{r}), g^{2c}(\boldsymbol{r})\big)d^3\boldsymbol{r}. \tag{37}$$

This results in our amfX2C picture-change correction to the xc energy,

$$\Delta \tilde{E}_{xc}^{2c} \simeq \Delta \tilde{E}_{xc,\oplus}^{2c} = \sum_{K=1}^{M} \big(\tilde{E}_{xc;K}^{2c} - E_{xc;K}^{2c}\big). \tag{38}$$

At first sight, this looks like a rather poor approximation, since, clearly,

$$\sum_K \tilde{E}_{xc;K}^{2c} = \sum_K \int \varepsilon_{xc}^{GGA}\big(\tilde{n}_K^{2c}(\boldsymbol{r}), \tilde{g}_K^{2c}(\boldsymbol{r})\big)d^3\boldsymbol{r}$$

$$\neq \int \varepsilon_{xc}^{GGA}\left(\sum_K \tilde{n}_K^{2c}(\boldsymbol{r}), \sum_K \tilde{g}_K^{2c}(\boldsymbol{r})\right)d^3\boldsymbol{r}, \tag{39}$$

due to the general nonlinear form of the xc functionals. However, we are calculating picture-change *corrections* and, so, one may expect that points for which $\tilde{n}_K^{2c}(\boldsymbol{r}) - n_K^{2c}(\boldsymbol{r})$ deviates significantly from zero for some atomic species K do not overlap with equivalent points for any other species. Under such conditions, our approximation becomes perfectly valid due to the local *ansatz* of the energy density ε_{xc}, cf. Eq. (24).

2. The noncollinear open-shell case

So far, we have discussed the KS amfX2C approach for a closed-shell molecular system characterized by a time-reversal symmetric density matrix. Due to the symmetry, the entire dependence of the exchange–correlation energy density reduces for a local-density approximation (LDA) only to the number density (n) [see Eq. (21)], for a generalized gradient approximation (GGA) also to its gradient, $g_{nn} \equiv (\nabla n) \cdot (\nabla n)$.

The situation is more complex for open-shell systems, where a general Kramers-unrestricted formalism results in a density matrix that has both the time-reversal symmetric (TRS) and time-reversal antisymmetric (TRA) components.[6,58] In fact, the latter component gives rise to a nonzero electron spin density, whose z-component (s_z) enters together with its gradient (∇s_z) into the nonrelativistic exchange–correlation energy expression, i.e., $\varepsilon_{xc}^{\text{GGA}} \equiv \varepsilon_{xc}^{\text{GGA}}(\{\rho r\}), \rho = n, g_{nn}, s_z, (\nabla s_z \cdot \nabla s_z), (\nabla n \cdot \nabla s_z)$.

However, the presented parametrization of the exchange–correlation energy involving only the z-component of the electron spin density and its gradient is inadequate for theories including the spin–orbit interaction, since the spatial and spin degrees of freedom are no longer independent. Their coupling results in a lack of rotational invariance of the exchange–correlation energy if only z spin-components are involved. This variance can be circumvented by a *noncollinear* parametrization/generalization of the nonrelativistic exchange–correlation energy density.

A common noncollinear *ansatz* follows earlier LDA-based works of Kubler *et al.*,[59] Sandratskii,[60] and van Wuellen[61] where the variable s_z is replaced by its corresponding magnitude $|s|$. Although this extension possesses no numerical problems in the evaluation of exchange–correlation energy, noncollinear potentials and kernels derived from GGA-type functionals are prone to numerical instabilities.[58] A more recent approach, which has been adopted in this work, is based on the noncollinear *ansatz* proposed by Scalmani and Frisch,[62] where variables depending on the z quantization axis are substituted by more adequate rotationally invariant counterparts,

$$s_z \to s \equiv |s|; \quad (\nabla s_z) \cdot (\nabla s_z) \to g_{ss} \equiv \sum_k (\nabla s_k) \cdot (\nabla s_k);$$
$$(\nabla n) \cdot (\nabla s_z) \to g_{ns} \equiv f_\nabla g. \tag{40}$$

Here, $k \in x, y, z$, $g \equiv |g|$ with $g_k = (\nabla n) \cdot (\nabla s_k)$, and $f_\nabla = \text{sgn}(g \cdot s)$. The noncollinear exchange–correlation energy then reads

$$E_{xc} = \int \varepsilon_{xc}^{\text{GGA}}(\{\rho r\}) d^3 r, \quad \rho = n, g_{nn}, s, g_{ss}, g_{ns}, \tag{41}$$

whereas the noncollinear exchange–correlation potential has the form[58]

$$F_{\mu\nu}^{\text{xc}} = \frac{dE_{xc}}{dD_{\nu\mu}} = \int \left(v_{xc}^n \Omega_{\mu\nu}^0 + v_{xc}^s \sum_k \frac{s_k}{s} \Omega_{\mu\nu}^k \right.$$
$$+ 2v_{xc}^{g_{nn}} \sum_k (\nabla_k n) \nabla_k \Omega_{\mu\nu}^0 + 2v_{xc}^{g_{ss}} \sum_{k,l} (\nabla_l s_k) \nabla_l \Omega_{\mu\nu}^k$$
$$\left. + v_{xc}^{g_{ns}} \sum_{k,l} f_\nabla \frac{g_k}{g} \left[(\nabla_l s_k) \nabla_l \Omega_{\mu\nu}^0 + (\nabla_l n) \nabla_l \Omega_{\mu\nu}^k \right] \right) d^3 r. \tag{42}$$

Here, $k, l \in x, y, z$ and v_{xc}^ρ refer to the partial derivative of $\varepsilon_{xc}^{\text{GGA}}$ with respect to $\rho \in n, g_{nn}, s, g_{ss}, g_{ns}$. $\Omega_{\mu\nu}^0$ and $\Omega_{\mu\nu}^k$ stand for the overlap and spin distribution functions, respectively, the latter being defined similarly to $\Omega_{\mu\nu}^0$ in Eq. (6) as

$$\Omega_{\mu\nu}^k(r) \equiv \chi_\mu^\dagger(r) \hat{\Sigma}_k \chi_\nu(r) \tag{43}$$

and involving components of the electron spin operator $\hat{\boldsymbol{\Sigma}}$.[58] Note that the evaluation of the exchange–correlation potential in Eq. (42) requires special attention to the limiting cases when the s or g functions approach zero. A detailed description of such a procedure is given in Ref. 58.

C. Extended amfX2C Hamiltonian

Having introduced the amfX2C scheme for both HF and KS mean-field theories, let us conclude this theory section by commenting on some important aspects of the amfX2C scheme, as well as comparing it to existing models for 2ePCE corrections. Ultimately, the discussion leads to the introduction of an extended amfX2C model, dubbed eamfX2C, which has the potential to outperform the amfX2C model, for instance, in properly treating long-range Coulomb interactions in solids.

We start by noting that (i) in contrast to Liu and Cheng,[34] our amfX2C scheme allows to take into account PCE corrections for both *spin-independent* and *spin-dependent* parts of the two-electron interaction; (ii) the proposed amfX2C approach has the additional appealing feature that it allows its straightforward extension to a KS-DFT framework as discussed in Sec. II B; (iii) the algebraic nature of amfX2C also allows an easy extraction of 2ePCE corrections not only from the common 2e Coulomb interaction term but also from more elaborate Gaunt and Breit 2e-interaction terms; and (iv) the 2ePCE corrections are only introduced in the atomic diagonal blocks. This further implies the following:

- The 2ePCE corrections will not contribute to the molecular gradient.
- The direct 2e Coulomb contribution will not cancel exactly the electron–nucleus interaction at long distance from atomic centers, which potentially prevents a direct application of amfX2C in solid-state calculations. This issue was discussed, for instance, by van Wüllen and Michauk and solved by building the former contributions using a superposition of atomic model densities,[41] although such a scheme does not accommodate HF exchange contributions.

In order to overcome the latter, particular shortcoming of the amfX2C model, we additionally propose a modified amfX2C model that exploits a superposition of atomic density matrices (expressed in AO-basis). The resulting *extended* amfX2C model (eamfX2C) is summarized in Algorithm 2. Most importantly, in contrast to the amfX2C model, where we assemble a molecular 4c Fock matrix $\boldsymbol{F}_\oplus^{\text{4c}}$ from atomic building blocks (see line 8 in Algorithm 1), this task is replaced in the eamfX2C algorithm by the buildup of a molecular *density* matrix $\boldsymbol{D}_\oplus^{\text{4c}}$ from atomic density matrices as indicated in line 10 of Algorithm 2. The latter construction, therefore, entails the evaluation of a two-electron (KS-)Fock matrix contribution in

Algorithm 2. Pseudo-code highlighting the essential steps for the eamfX2C approach.

1: /* Initialize the molecular effective density matrices */

2: $\boldsymbol{D}_{\oplus}^{4c} = \boldsymbol{0}$; $\tilde{\boldsymbol{D}}_{\oplus}^{2c} = \boldsymbol{0}$

3: **for all** unique atom types $K \in$ molecule **do**

4: Let $\{\mu, \nu\} \in$ atomic basis K

5: /* Solve the 4c SCF equation */

6: $\boldsymbol{F}_K^{4c}\boldsymbol{c}_K^{4c} = \boldsymbol{c}_K^{4c}\boldsymbol{\epsilon}_K^{4c}$ with $F_{K,\mu\nu}^{4c} = \begin{cases} F_{K,\mu\nu}^{4c,\mathrm{HF}}[\boldsymbol{D}_K^{4c}] = h_{K,\mu\nu}^{4c} + \sum\limits_{\gamma,\delta\in K} G_{\mu\nu,\gamma\delta}^{4c}D_{K,\delta\gamma}^{4c} \\ F_{K,\mu\nu}^{4c,\mathrm{KS}}[\boldsymbol{D}_K^{4c}] = h_{K,\mu\nu}^{4c} + \sum\limits_{\gamma,\delta\in K} G_{\mu\nu,\gamma\delta}^{\omega,4c}D_{K,\delta\gamma}^{4c} + F_{K,\mu\nu}^{4c,\mathrm{xc}}[\boldsymbol{D}_K^{4c}] \end{cases}$

7: /* Evaluate the atomic X2C decoupling matrix $\boldsymbol{U}_K$ from $\boldsymbol{F}_K^{4c}$ and calculate */

8: $\tilde{\boldsymbol{D}}_K^{2c} = \left[\boldsymbol{U}_K^\dagger \boldsymbol{D}_K^{4c} \boldsymbol{U}_K\right]^{\mathrm{LL}}$

9: /* Add K-th atomic effective density matrices $\boldsymbol{D}_K^{4c}$ and $\tilde{\boldsymbol{D}}_K^{2c}$ to the molecular block */

10: $\boldsymbol{D}_{\oplus}^{4c} \leftarrow \boldsymbol{D}_K^{4c}$; $\tilde{\boldsymbol{D}}_{\oplus}^{2c} \leftarrow \tilde{\boldsymbol{D}}_K^{2c}$

11: **end for**

12: Let $\{\mu, \nu\} \in$ full molecular basis

13: /* Evaluate the molecular 4c 2e Fock matrix $\boldsymbol{F}_{\oplus}^{4c,\,2e}$ with elements */

14: $F_{\oplus,\mu\nu}^{4c,\,2e} = \begin{cases} F_{\oplus,\mu\nu}^{4c,2e,\mathrm{HF}}[\boldsymbol{D}_{\oplus}^{4c}] = \sum\limits_{\gamma,\delta} G_{\mu\nu,\gamma\delta}^{4c}D_{\oplus,\delta\gamma}^{4c} \\ F_{\oplus,\mu\nu}^{4c,2e,\mathrm{KS}}[\boldsymbol{D}_{\oplus}^{4c}] = \sum\limits_{\gamma,\delta} G_{\mu\nu,\gamma\delta}^{\omega,4c}D_{\oplus,\delta\gamma}^{4c} + F_{\mu\nu}^{4c,\mathrm{xc}}[\boldsymbol{D}_{\oplus}^{4c}] \end{cases}$

15: /* If DFT, evaluate also the molecular xc energy $E_{xc}^{4c}[\boldsymbol{D}_{\oplus}^{4c}]$ */

16: /* Evaluate the molecular X2C decoupling matrix $\boldsymbol{U}$ from */

17: $\tilde{\boldsymbol{h}}^{4c} = \boldsymbol{h}^{4c} + \boldsymbol{F}_{\oplus}^{4c,\,2e}$

18: /* Determine the molecular 2e picture-change transformation correction as */

19: $\Delta\tilde{\boldsymbol{F}}_{\oplus}^{2c,\,2e} = \left[\boldsymbol{U}^\dagger \boldsymbol{F}_{\oplus}^{4c,\,2e} \boldsymbol{U}\right]^{\mathrm{LL}} - \boldsymbol{F}^{2c,\,2e}$

20: where

21: $F_{\mu\nu}^{2c,\,2e} = \begin{cases} F_{\mu\nu}^{2c,2e,\mathrm{HF}}[\tilde{\boldsymbol{D}}_{\oplus}^{2c}] = \sum\limits_{\gamma,\delta} G_{\mu\nu,\gamma\delta}^{2c}\tilde{D}_{\oplus,\delta\gamma}^{2c} \\ F_{\mu\nu}^{2c,2e,\mathrm{KS}}[\tilde{\boldsymbol{D}}_{\oplus}^{2c}] = \sum\limits_{\gamma,\delta} G_{\mu\nu,\gamma\delta}^{\omega,2c}\tilde{D}_{\oplus,\delta\gamma}^{2c} + F_{\mu\nu}^{2c,\mathrm{xc}}[\tilde{\boldsymbol{D}}_{\oplus}^{2c}] \end{cases}$

22: /* If DFT, determine also the molecular PCE correction to the xc energy as */

23: $\Delta\tilde{E}_{xc,\oplus}^{2c} = E_{xc}^{4c}[\boldsymbol{D}_{\oplus}^{4c}] - E_{xc}^{2c}[\tilde{\boldsymbol{D}}_{\oplus}^{2c}]$

24: /* Solve the 2c SCF equation with the eamfX2C Fock matrix operator */

25: $\boldsymbol{F}^{2c}\boldsymbol{c}^{2c} = \boldsymbol{c}^{2c}\boldsymbol{\epsilon}^{2c}$ with $F_{\mu\nu}^{2c} \equiv F_{\mu\nu}^{\mathrm{eamfX2C}} = \underbrace{\left[\boldsymbol{U}^\dagger \boldsymbol{h}^{4c} \boldsymbol{U}\right]_{\mu\nu}^{\mathrm{LL}} + \Delta\tilde{F}_{\oplus,\mu\nu}^{2c,\,2e}}_{\text{static terms}} + \underbrace{F_{\mu\nu}^{2c,\,2e}[\boldsymbol{D}^{2c}]}_{\text{dynamic term}}$

---

the *full* molecular basis within a 4c framework (cf. line 14 of Alg.2), which is absent in the molecular computational panel (lower part of Algorithm 1) of the simpler amfX2C model. Although introducing such a requirement seems odd at a first glance, in particular, with regard to computational scaling, let us recall that an efficient density-based screening in the two-electron (KS-)Fock matrix construction will enable a calculation of the term $F_{\mu\nu}^{4c,\,2e}[\boldsymbol{D}_{\oplus}^{4c}]$ at a fractional cost of a regular two-electron (KS-)Fock matrix evaluation because of the sparsity associated with the molecular density matrix $\boldsymbol{D}_{\oplus}^{4c}$. In this regard, one can recognize a similarity between the eamfX2C scheme and the atomic initial guess proposed by van Lenthe and co-workers[63] where the initial Fock matrix is formed from a superposition of atomic density matrices. Moreover, in the KS-DFT framework, one can also easily obtain the xc energy picture-change correction (Algorithm 2, line 23) from contributions evaluated in the full *molecular* basis,

$$\Delta\tilde{E}_{xc}^{2c} \simeq \tilde{E}_{xc,\oplus}^{2c} = E_{xc}^{4c}[\boldsymbol{D}_{\oplus}^{4c}] - E_{xc}^{2c}[\tilde{\boldsymbol{D}}_{\oplus}^{2c}], \qquad (44)$$

in contrast to the correction term $\Delta\tilde{E}_{xc}^{2c}$ of the amfX2C model (Algorithm 1, line 14), which consists of a sum of K contributions each calculated in the Kth *atomic* basis.

D. A remark on notations

Since the combination of a several 2ePCE correction models with multiple defining Hamiltonians for obtaining the unitary decoupling matrix $\boldsymbol{U}$ may easily lead to confusion, we have decided to introduce a notation for X2C Hamiltonians where the 2ePCE correction model is given as a prefix "a" while the defining Hamiltonian matrix $\boldsymbol{h}_{\mathrm{def}}^{4c}$ is given as subscript b, that is, aX2C$_b$.

In particular, we have

$$a = \begin{cases} \text{1e} & \textbf{if no 2ePCE corrections added:} \ \Delta \tilde{F}^{2c,2e} = \mathbf{0} \\ \text{amf} & \textbf{if atomic–mean field 2ePCE corrections added:} \ \Delta \tilde{F}^{2c,2e} \simeq \Delta \tilde{F}_{\oplus}^{2c,2e} \ \text{(see line 14 in Alg. 1)} \\ \text{eamf} & \textbf{if extended atomic–mean field 2ePCE corrections added:} \ \Delta \tilde{F}^{2c,2e} \simeq \Delta \tilde{F}_{\oplus}^{2c,2e} \ \text{(see line 19 in Alg. 2)} \\ \text{AMFI} & \textbf{if atomic–mean field first–order (DKH1) spin–orbit 2ePCE corrections added:} \ \text{see Refs. 37 and 38} \\ \text{mmf} & \textbf{if post–SCF molecular–mean field 2ePCE corrections added:} \ \text{see Ref. 32} \end{cases}$$

and

$$b = \begin{cases} \text{D} & \textbf{if } U \textbf{ is evaluated from } h_{\text{def}}^{4c} \equiv h^{4c} \textbf{ where } h^{4c} \textbf{ is the one–electron Dirac Hamiltonian} \\ \text{DC} & \textbf{if } U \textbf{ is evaluated from } h_{\text{def}}^{4c} \equiv h^{4c} + F_{\oplus}^{4c,2e} \textbf{ with } \underline{C}\text{oulomb integrals contributing to } F_{\oplus}^{4c,2e} \\ \text{DCG} & \textbf{if } U \textbf{ is evaluated from } h_{\text{def}}^{4c} \equiv h^{4c} + F_{\oplus}^{4c,2e} \textbf{ with } \underline{C}\text{oulomb–}\underline{G}\text{aunt integrals contributing to } F_{\oplus}^{4c,2e} \\ \text{DCB} & \textbf{if } U \textbf{ is evaluated from } h_{\text{def}}^{4c} \equiv h^{4c} + F_{\oplus}^{4c,2e} \textbf{ with } \underline{C}\text{oulomb–}\underline{B}\text{reit integrals contributing to } F_{\oplus}^{4c,2e}. \end{cases}$$

III. COMPUTATIONAL DETAILS

If not stated otherwise, all calculations reported in this work have been carried out by both DIRAC[5] and RESPECT[6] programs, making use of a common computational setup: (i) a finite value for the speed of light $c = 137.035\,999\,074\,00\ a_0 E_h/\hbar$,[64] (ii) a point nucleus model for all atomic nuclei to ease comparison between data obtained by the programs, (iii) an explicit inclusion of $(SS|SS)$-type electron-repulsion AO integrals, (iv) atom-centered uncontracted Gaussian-type basis sets of double-ζ quality (dyall.v2z, dubbed v2z) for each unique atom type,[65–72] (v) DIRAC's default numerical integration grids consisting of the basis-set adaptive radial quadrature by Lindh et al.,[73] and the angular quadrature by Lebedev[74–76] (to achieve consistent exchange–correlation PCE corrections by both programs, it turned out be crucial to use integration grids of identical composition and quality), and (vi) a threshold for SCF convergence of 10^{-7} in the error vector of the direct inversion of the iterative subspace (DIIS)[77] algorithm DIIS[77]. All atomic and molecular

calculations with DIRAC were performed within a Kramers-restricted (KR) formalism, employing for open-shell systems either an average-of-configuration (AOC) approach[53] (HF) or a fractional occupation (FO) approach (KS-DFT). In the case of group 16 diatomics (chalcogenide series), AOC-HF calculations take into account all possible configurations of six electrons in eight Kramers-paired spinors (i.e., representing the π, π^* valence shells). In RESPECT, molecular open-shell calculations were performed within a Kramers-unrestricted (KU) formalism,[6] whereas atomic results were obtained with the KR FO approach, both for HF and for KS-DFT calculations. All KS-DFT calculations were carried out with either a PBE or PBE0 exchange–correlation functional.[78–80]

For the lighter noble gas dimers, internuclear distances were taken from experimentally available data[81] whereas for the heavier homologues Rn_2 and Og_2, respectively, computationally optimized structures were taken from Ref. 82. Similarly, in the case of the chalcogen series, all geometries were taken from Ref. 83, except for the heaviest diatomic system Lv_2 for which the internuclear distance
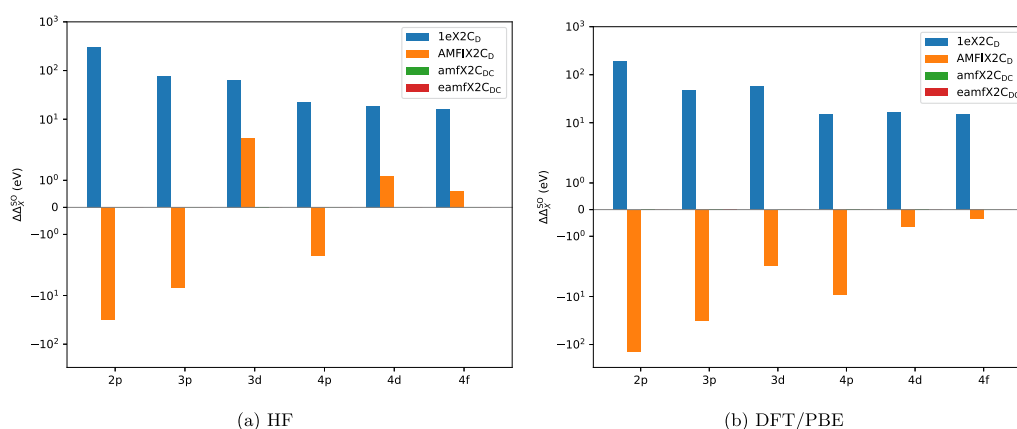
FIG. 1. Differences of spin–orbit splittings (Δ_X^{SO}) of the inner-core to outer-core Og-atomic-like shells in Og_2 with respect to the ^4DC reference values within either an HF approach [panel (a)] or a DFT/PBE approach [panel (b)]. All data are compiled from the SCF spinor energies listed in Tables II and III, respectively. Energy differences are given in eV. Note that errors associated with the (e)amfX2C models are not visible in the figures.

of $R_e = 3.230$ Å was extracted by visual inspection from Fig. 1 of Ref. 84. Table I summarizes the structural parameters for all group 16 and group 18 diatomics employed in this work.

In the case of the methane molecule CH_4 discussed in Sec. IV A 3, we assumed a T_d-symmetrical molecular framework with a C–H internuclear distance of 1.091 Å and a <H–C–H bond angle of 109.471°. In order to enhance relativistic effects, we scaled down the speed of light c by a factor of 10, corresponding to an actual value of $c_{scaled} = 13.703\,599\,907\,400\ a_0 E_h/\hbar$, for both the atomic as well as the molecular calculations.

The absolute contact densities and contact density shifts for selected (closed-shell) copernicium fluorides (CnF_n, $n = 0, 2, 4, 6$), discussed in Sec. IV B, were calculated from mean-field HF wave functions employing a 4c Dirac–Coulomb as well as the X2C Hamiltonian supplemented with various 2ePCE corrections. The structures for each of the copernicium fluorides were optimized within a 4c Dirac–Coulomb framework by means of KS-DFT calculations employing the PBE0 exchange–correlation functional. Following the very recent work of Hu and Zou,[85] we assumed for the structure optimization a linear ($n = 2$), square-planar ($n = 4$), and octahedral ($n = 6$) geometry for the respective copernicium fluorides CnF_n. The resulting equilibrium Cn–F internuclear distances are compiled in Table X along with the corresponding double group symmetry. It is worth noting that, given that the primary concern of our the present study is not to provide an accurate computation of the contact density with respect to a converged basis-set saturation at the heavy nuclei Cn, we did not pursue any further augmentation of the set of primitives in the basis set as, for example, done in our earlier works in Refs. 86 and 87. Moreover, as we aim within the e(amf)X2C models to reproduce as accurately as possible the parent four-component results, computational details for the two-component calculations have to match the corresponding ones for four-component reference calculations. Hence, any consideration for convergence in the basis set, crucial to obtain quantitatively converged contact densities, holds simultaneously in both cases: in a four-component and a two-component framework.

Finally, Sec. IV C comprises an assessment of the accuracy and suitability of various 2c approaches to adequately describe (absolute) K- and L-edge core-ionization energies as well as L_3-L_2-edge spin–orbit splittings, denoted as Δ_L^{SO}, for heavy d- and p-block compounds. To this end, we considered one atomic anion (At^-)

and two anionic and neutral molecular cases, respectively. In the former case, we employed the same computational setup for the SCF and equation-of-motion coupled-cluster singles-and-doubles (EOM-CCSD[88]) calculations as described in full detail in Ref. 89, which provides high-quality computational reference data. In the remaining molecular examples, we employed for CnF_6 the optimized molecular structure listed in Table X, while for $[Au(Cl)_4]^-$ the optimized molecular structure has been taken from Table I (column MP2/aug-cc-pVTZ) in Ref. 90. In either molecular case, we correlated for the EOM-CCSD step all electrons and introduced an energy-based cutoff in the virtual spinor space at 3 Hartree making use of the dyall.v2z basis sets for all atom types. Since we are solely interested in a genuine comparison of different two-component Hamiltonian models rather than achieving *quantitatively converged* results for the K-edge, L-edge, and M-edge (the latter only for the [Au]-complex) ionization potentials, which would require, for example, to make use of tailored basis sets,[91] the latter motivates for the present work our choice to merely aim at a *qualitative* electron correlation treatment.

IV. RESULTS AND DISCUSSION

In this section, we will critically assess the accuracy of our newly developed 2ePCE correction approaches for all-electron X2C HF and DFT calculations in the two major, common-use cases: (i) with a variational account of SO interaction and (ii) in a genuine spinfree SC framework. A detailed summary of the notation of the 2ePCE correction applied to the X2C Hamiltonian can be found in Sec. II D.

In Sec. IV A, we commence with a discussion of the spinor energies of Og_2, a prototypical, closed-shell superheavy diatomic molecule, optimized both within a mean-field HF and a KS-DFT computational model (Sec. IV A 1). Results for the lighter homologues of the corresponding group 18 diatomics can be found in the public research repository ZENODO (see Sec. V for more details). Along the same lines and as an example of an open-shell diatomic molecule, we consider in Sec. IV A 2 the case of Te_2 as a representative of the group 16 diatomics. Results for the remaining group 16 diatomics listed in Table I can also be found in the ZENODO repository (see Data Availability for more details). To conclude the discussion on total as well as spinor energies, we assess in Sec. IV A 3 the numerical performance of our selection of PCE-corrected X2C models for the case of an "ultrarelativistic" methane molecule employing a ten-fold reduced speed of light c, that is, $c/10$.

Next, in Sec. IV B, we evaluate the suitability of our (e)amf-X2C models for the calculation of absolute contact densities at a heavy nuclear center and, equally important, for contact density *shifts*. The latter play, for example, an important role in computational models for the determination of isomer shifts that are accessible in experimental Mössbauer spectroscopy. To this end, we perform contact density calculations for a series n (with $n = 0, 2, 4, 6$) of fluoride compounds of the heaviest group 12 member Cn, ranging from the bare Cn atom to the hexafluoride CnF_6.

In Sec. IV C, we conclude our assessment by focusing on the calculation of correlated x-ray core-ionization energies. Besides the At^- mono-anion for which benchmark data are available in the literature,[89] we consider two molecular applications of 5d- and 6d-containing molecules by taking advantage of the recently developed EOM-CCSD approach for core spectroscopy.[89]

TABLE I. Structural parameters of the group 16 (left-hand side) and group 18 diatomics (right-hand side) considered in this work. All internuclear distances are given in Å.

Molecule	$r_{X–X}$	Reference	Molecule	$r_{X–X}$	Reference
			He_2	2.970	81
O_2	1.207 52	83	Ne_2	3.091	81
S_2	1.889	83	Ar_2	3.756	81
Se_2	2.166	83	Kr_2	4.008	81
Te_2	2.557	83	Xe_2	4.363	81
Po_2	2.795	83	Rn_2	4.427	82
Lv_2	3.230	84	Og_2	4.329	82

A. Spinor energies of (super)heavy diatomic molecules

1. Closed-shell Og₂

In the following, we will assess the numerical performance of our atomic mean-field PCE correction model and its extended version within the context of an exact two-component decoupling approach by considering as prime example the heaviest group 18 dimer, viz., Og_2. Since the molecule is closed-shell in its electronic ground state, both the Kramers-restricted and the Kramers-unrestricted SCF formalism implemented in DIRAC and RESPECT, respectively, converge to the same solution. In order to underline the importance of a simultaneous treatment of 2eSC and 2eSO PCE corrections within the X2C Hamiltonian framework, we compile in Table II a selected set of HF spinor energies for Og_2, ranging from the inner-core to the outer-core as well as to the valence region, and we compare the various X2C-based spinor energies with the 4c Dirac–Coulomb reference data (^{4}DC; sixth column in Table II). In addition, the left panel of Fig. 1 comprises the HF-based deviations for SO splittings of the inner-core and outer-core shells of Og_2 with predominant atomic-like character illustrated for results obtained with the various two-component Hamiltonian schemes

listed in Table II by comparison to the ^{4}DC reference. Finally, the right panel of Fig. 1 provides a similar comparison for a correlated KS-DFT-based approach employing the PBE functional where the underlying absolute energies are summarized in Table III.

a. HF. In line with previous studies,[31,41] we find the largest deviations within an X2C framework from the reference 4c spinor energies in an HF approach for the innermost s and p shells where 2eSO (p shells) and 2eSC PCE corrections (s and p shells) are expected to be of utmost importance (see also the discussion of core-ionization energies in Sec. IV C). Hence, considering first the bare one-electron X2C (second column, 1eX2C$_D$ in Table II), which ignores 2e picture changes altogether, we encounter deviations up to +23.8 Hartree with respect to the four-component reference data for the innermost s shells and up to −7.2 Hartree for the lowest-lying p shells. Next, taking into account atomic SO mean-field PCE corrections within the AMFI model (third column, AMFIX2C$_D$) results in a minor improvement of about −0.4 Hartree for the inner s shells while the lowest-lying p shells become destabilized through the PCE corrections by about +10 Hartree, leading to a deviation of ≈ +2.7 Hartree with respect to the corresponding 4c reference values.

TABLE II. SCF total energy (E) and spinor energies of selected doubly degenerate occupied spinors (ϵ) for Og_2 as obtained from HF/v2z calculations within a four-component Dirac–Coulomb (^{4}DC) as well as a two-component Hamiltonian framework, including the new (e)amfX2C$_{DC}$ models. All energies are given in Hartree.

	1eX2C$_D$	AMFIX2C$_D$	amfX2C$_{DC}$	eamfX2C$_{DC}$	^{4}DC
E	−110 045.256 93	−110 015.966 88	−110 116.091 02	−110 116.091 02	−110 116.091 01
ϵ_{1-2}	−8248.362 74	−8248.695 05	−8272.125 30	−8272.125 29	−8272.125 29
ϵ_{3-4}	−1733.891 54	−1734.001 01	−1738.997 64	−1738.997 63	−1738.997 63
ϵ_{5-6}	−1693.296 07	−1683.361 33	−1686.063 74	−1686.063 74	−1686.063 74
ϵ_{7-10}	−1133.936 51	−1136.418 86	−1137.979 05	−1137.979 04	−1137.979 04
ϵ_{11-12}	−474.973 49	−475.013 15	−476.180 10	−476.180 10	−476.180 10
ϵ_{13-14}	−454.670 04	−452.301 45	−452.933 31	−452.933 31	−452.933 31
ϵ_{15-18}	−317.105 73	−317.769 56	−318.141 42	−318.141 42	−318.141 42
$\epsilon_{19,-,22}$	−287.847 02	−286.460 16	−286.468 62	−286.468 61	−286.468 61
ϵ_{23-28}	−264.511 00	−265.355 39	−265.514 76	−265.514 76	−265.514 76
$\epsilon_{29,-,30}$	−142.096 99	−142.111 36	−142.432 46	−142.432 46	−142.432 46
ϵ_{31-32}	−131.900 02	−131.201 72	−131.364 62	−131.364 62	−131.364 62
ϵ_{33-36}	−91.647 27	−91.851 15	−91.948 18	−91.948 18	−91.948 18
ϵ_{37-40}	−76.613 48	−76.208 53	−76.196 82	−76.196 82	−76.196 82
ϵ_{41-46}	−70.008 92	−70.257 53	−70.287 99	−70.287 99	−70.287 99
ϵ_{47-52}	−50.088 77	−49.760 60	−49.737 04	−49.737 03	−49.737 03
ϵ_{53-60}	−47.748 19	−47.990 85	−47.990 04	−47.990 04	−47.990 04
...	...	...	...	...	...
ϵ_{110}	−1.470 90	−1.482 71	−1.481 61	−1.481 62	−1.481 62
ϵ_{111}	−1.313 83	−1.313 14	−1.316 99	−1.316 98	−1.316 98
ϵ_{112}	−1.312 54	−1.311 85	−1.315 72	−1.315 71	−1.315 71
ϵ_{113}	−0.746 47	−0.737 30	−0.738 19	−0.738 19	−0.738 19
ϵ_{114}	−0.743 81	−0.734 55	−0.735 45	−0.735 45	−0.735 45
ϵ_{115}	−0.316 91	−0.318 26	−0.318 21	−0.318 22	−0.318 22
ϵ_{116}	−0.303 72	−0.305 16	−0.305 12	−0.305 12	−0.305 12
ϵ_{117}	−0.292 60	−0.294 13	−0.294 11	−0.294 11	−0.294 11
ϵ_{118}	−0.280 36	−0.281 96	−0.281 94	−0.281 93	−0.281 93

TABLE III. SCF total energy (E) and spinor energies (ϵ) of the doubly degenerate occupied spinors for Og$_2$ as obtained from DFT/PBE/v2z calculations within a four-component Dirac–Coulomb (^{4}DC) as well as a two-component Hamiltonian framework, including the new (e)amfX2C$_{DC}$ models. All energies are given in Hartree.

	1eX2C$_D$	AMFIX2C$_D$	amfX2C$_{DC}$	eamfX2C$_{DC}$	^{4}DC
E	−110 101.192 89	−110 071.817 03	−110 191.687 17	−110 191.687 17	−110 191.687 16
ϵ_{1-2}	−8194.400 21	−8194.743 58	−8228.578 26	−8228.578 26	−8228.578 26
ϵ_{3-4}	−1714.663 79	−1714.767 64	−1720.619 64	−1720.619 64	−1720.619 64
ϵ_{5-6}	−1675.008 48	−1665.139 58	−1672.435 70	−1672.435 70	−1672.435 70
ϵ_{7-10}	−1119.860 23	−1122.324 02	−1124.503 68	−1124.503 67	−1124.503 67
ϵ_{11-12}	−465.421 15	−465.455 60	−466.742 89	−466.742 89	−466.742 89
ϵ_{13-14}	−445.526 84	−443.183 39	−444.878 50	−444.878 50	−444.878 49
ϵ_{15-18}	−309.804 99	−310.459 33	−310.944 33	−310.944 33	−310.944 33
$\epsilon_{19,-,22}$	−281.438 39	−280.068 78	−280.357 30	−280.357 30	−280.357 30
ϵ_{23-28}	−258.404 60	−259.237 60	−259.442 79	−259.442 79	−259.442 79
$\epsilon_{29,-,30}$	−137.014 95	−137.026 61	−137.366 44	−137.366 44	−137.366 44
ϵ_{31-21}	−127.091 44	−126.403 62	−126.860 89	−126.860 89	−126.860 89
ϵ_{33-26}	−87.691 23	−87.889 59	−88.004 19	−88.004 18	−88.004 18
ϵ_{37-40}	−73.278 01	−72.881 07	−72.934 37	−72.934 37	−72.934 37
ϵ_{41-46}	−66.867 98	−67.111 11	−67.140 79	−67.140 78	−67.140 78
ϵ_{47-52}	−47.780 11	−47.458 64	−47.455 76	−47.455 76	−47.455 76
ϵ_{53-60}	−45.500 42	−45.737 73	−45.722 33	−45.722 33	−45.722 33
$\cdots$	$\cdots$	$\cdots$	$\cdots$	$\cdots$	$\cdots$
ϵ_{110}	−1.165 75	−1.176 60	−1.174 08	−1.174 09	−1.174 09
ϵ_{111}	−1.005 57	−1.005 35	−1.007 95	−1.007 95	−1.007 95
ϵ_{112}	−1.004 85	−1.004 63	−1.007 24	−1.007 24	−1.007 24
ϵ_{113}	−0.541 22	−0.533 07	−0.536 04	−0.536 03	−0.536 03
ϵ_{114}	−0.539 07	−0.530 85	−0.533 84	−0.533 84	−0.533 84
ϵ_{115}	−0.209 29	−0.210 28	−0.210 07	−0.210 07	−0.210 07
ϵ_{116}	−0.199 42	−0.200 48	−0.200 27	−0.200 27	−0.200 27
ϵ_{117}	−0.191 01	−0.192 15	−0.191 94	−0.191 94	−0.191 94
ϵ_{118}	−0.183 04	−0.184 21	−0.184 01	−0.184 00	−0.184 00

By contrast, both our amfX2C$_{DC}$ and eamfX2C$_{DC}$ PCE correction schemes for the X2C Hamiltonian yield spinor energies that merely differ by 10 μHartree or less for the innermost s shells—and likewise for the p shells—of Og$_2$ from the 4c reference data. These findings strikingly illustrate the excellent numerical performance of our newly proposed amf-based 2eSC- and 2eSO-PCE corrections applied in a molecular framework. Moreover, in particular in the core region close to a (heavy) nucleus, SO splittings are a crucial measure since they probe the ability of PCE-corrected 2c schemes to provide *quantitative relative* energies. Here, calculations employing the 1eX2C$_D$ as well as the AMFIX2C$_D$ Hamiltonian yield SO splittings for the atomic-like shells (Δ_X^{SO}, $X = p, d, f$ obtained as energy difference $\epsilon_{X_{(2l+1)/2}} - \epsilon_{X_{(2l-1)/2}}$) in Og$_2$, which deviate significantly from the ^{4}DC reference data as illustrated in Fig. 1(a) with data obtained from Table II. For example, for the bare 1eX2C$_D$ approach, we find deviations in Δ_X^{SO} of up to $\approx +11.3$ Hartree for the 2p shell, which corresponds to an overestimation of the splitting by $\approx$ 2%. Moving to outer-core shells, the overestimation of the SO splitting Δ^{SO} becomes even worse with deviations as large as $\approx$ +25% for Δ_{4f}^{SO}. As can be seen from Fig. 1(a), the latter deviations can be reduced significantly for all inner- and outer-core spin–orbit-split shells through the introduction of AMFI-based SO mean-field

PCE corrections within AMFIX2C$_D$. Finally, as it is evident from the matching *absolute* spinor energies discussed above, all SO splittings considered in Fig. 1(a) obtained within our (e)amfX2C$_{DC}$ Hamiltonian frameworks match (within significant digits) their 4c reference data (errors are, therefore, not visible in the figure), underlining once more the importance of taking into account both 2eSC- and 2eSO-PCE corrections in an X2C many-electron Hamiltonian framework.

In passing, we note that the numerical performance of our (e)amfX2C models not only holds for the inner- and outer-core but also for the corresponding valence shells ($\epsilon_{110-118}$ in Table II) of the diatomic Og$_2$ where the ^{4}DC and (e)amfX2C$_{DC}$ data essentially remain indistinguishable within significant digits. It is worth noting that in the (outer-)valence region, the AMFIX2C$_D$ approach leads to absolute spinor energies that differ by less than 10^{-3} Hartree from their reference values. Hence, the latter may explain why this PCE correction scheme has successfully been applied in the past in numerous numerical applications that particularly probed valence-dominated properties. Finally, our data in Table II further show that neglecting PCE corrections results even for valence spinors in absolute errors for the spinor energies on the order of 10^{-2} Hartree.

b. DFT/PBE. What about the numerical performance of our (e)amf PCE correction models in a correlated framework? To this end, we consider in the following the same prime superheavy diatomic molecular system Og_2 (*vide supra*) within a DFT/PBE-based SCF approach. A particularity of our (e)amf PCE correction models is rooted in the fact that, as illustrated in Algorithms 1 and 2, respectively, both models enable not only a basis-set dependent but also a *self-consistent-field model dependent* PCE correction that originates from the specific contributions entering the corresponding 2e Fock matrices. The latter implies that our (e)amf PCE correction models provide tailor-made PCE corrections that explicitly account for the subtleties arising from the employed exchange–correlation functional within a KS-DFT-based SCF approach. By contrast, to the best of our knowledge, common PCE schemes, such as the AMFI approach, do—by construction—*not* allow to distinguish between 2eSO PCE corrections for the X2C Hamiltonian that aim for either an ensuing (uncorrelated) 2c HF or (correlated) KS-DFT-based many-electron SCF calculation. Bearing these subtle, yet crucial, details in mind, the strikingly excellent numerical performance of our (e)amfX2C$_{DC}$ models with respect to the ^{4}DC reference spinor energies as well as total energies illustrated in Table III not only underlines the outstanding numerical performance of our newly proposed PCE correction *ansätze* but also perfectly agrees with our previous conclusions within the HF approach (*vide supra*). Moreover, the SO splittings Δ_X^{SO} of the (e)amfX2C$_{DC}$ and ^{4}DC cases match again exactly within significant digits for all the selected inner-core and outer-core atomic-like shells shown in Fig. 1(b). Notably, as indicated above, the (basis-set dependent) AMFI-based SO PCE corrections are SCF-model independent and, hence, strictly identical for both common use cases: an X2C-HF and X2C-KS-DFT approach. Consequently, AMFI does not include *a priori* any PCE correction on the SO splitting originating from amf *two-electron correlation effects*, which should primarily have an impact on the resulting splitting of the most strongly SO-split p shells. A close inspection of the left (HF) and right (DFT/PBE) panels of Fig. 1 reveals that the deviations from the ^{4}DC reference for Δ_X^{SO} ($X = 2p, 3p, 4p$) are indeed systematically larger in the (correlated) DFT/PBE case.

c. On the importance of two-electron scalar-relativistic PCE corrections. In the previous paragraphs, we discussed the performance of our newly proposed (e)amf PCE corrections for the X2C Hamiltonian in either a HF or KS-DFT framework with particular focus on *relative* spinor energies of the superheavy diatomic molecule Og_2, that is, for example, on the resulting SO splittings of inner- and outer-core atomic-like shells by comparison to the corresponding ^{4}DC reference data. In order to highlight the full potential of our (e)amf PCE models, let us recall that our 2ePCE correction models take into account both 2eSO *and* 2eSC correction terms. Whereas 2eSO PCE corrections are common to include in an (exact) two-component Hamiltonian framework for many-electron systems,[34,37,38,41] the inclusion of 2eSC-PCE correction terms is less so, despite their apparent significance to be illustrated in the following. To this end, we turn to a genuine spinfree SC framework by eliminating all spin-dependent terms from the parent ^{4}DC Hamiltonian by means of the Dirac relation.[33,92] Hence, the results obtained on the basis of the SC-^{4}DC Hamiltonian will serve as references for the discussion of the numerical performance of various

PCE-corrected SC-X2C Hamiltonian models. For the ease of comparison with the above spin-dependent data, we consider in Tables IV and V, respectively, in a spinfree *ansatz* the same superheavy diatomic molecule Og_2.

A close inspection of both tables first shows that the bare (no PCE corrections) SC-1eX2C$_D$ and the SC-AMFIX2C$_D$ Hamiltonians yield within either computational model, viz. HF and DFT/PBE, strictly matching numerical results. The reason is that with the elimination of any spin-dependent term from the (parent) 4c Hamiltonian, the AMFI PCE corrections simply become zero. Moreover, as could be expected, the largest 2eSC PCE corrections are encountered for the inner s shells (molecular spinors ϵ_{1-4} in Tables IV and V) with deviations for SC-1eX2C$_D$ ($\equiv$ SC-AMFIX2C$_D$) up to 27.2 Hartree in the HF and 35.3 Hartree in the DFT/PBE case compared to the SC-^{4}DC reference data. By moving to the outer-core and up to occupied molecular spinors close to the Fermi level, 2eSC PCEs start to fade significantly with absolute deviations for the HOMO and HOMO-1 amounting to less than 10^{-4} Hartree. By contrast, our SC-(e)amfX2C$_{DC}$ models provide an even higher numerical accuracy by at least one order of magnitude ($<10^{-5}$) for *all* occupied molecular spinors summarized in Tables IV and V, that is, ranging from the innermost s shells to the Fermi level. The latter findings, therefore, unequivocally illustrate that our atomic SC-(e)amfX2C$_{DC}$ PCE correction models are capable of efficiently correcting for 2ePCEs in a molecular framework. Consequently, this distinct asset of our (e)amfX2C models is a key ingredient for their above discussed numerical success in a spin-dependent Hamiltonian framework where 2eSC and 2eSO coupling contributions are both simultaneously at play and should not be considered on a different footing. In passing, we further note that also in the present spinfree case, the total SCF energies obtained within either our (e)amfX2C or a 4c Hamiltonian framework agree up to μ-Hartree accuracy, regardless of the underlying SCF *ansatz*.

2. Open-shell Te$_2$

In Sec. IV A 1, we primarily focused on the numerical assessment of various 2ePCE corrections schemes for the X2C Hamiltonian in a many-electron context on the basis of the closed-shell superheavy diatomic molecule Og_2. In particular, we paid attention to the capability of various 2ePCE-corrected X2C models to provide matching molecular spinor energies by comparison to four-component reference data. In the chemistry of (molecular compounds of) heavy and superheavy elements, one frequently has to cope with partially occupied electronic shells due to the possibility of unfilled s, p, d and/or f electronic shells. In order to showcase the versatility of our (e)amf PCE corrections for the X2C Hamiltonian also in such a context, we consider in the following the open-shell molecule Te$_2$. The latter system is a heavy homologue of O_2 and, for this reason, best characterized by a valence electronic structure that can be written in shorthand as $\pi_u^4 \pi_g^{*,2}$ (assuming an approximate yet more familiar spin–orbit-free notation of the molecular spinors). For a more detailed discussion of the electronic structure of the homonuclear diatomic systems of group 16 ranging from O_2 to Po_2, we refer the reader, for example, to Ref. 83. As shown in the latter, the molecular bonding (π_u) and antibonding (π_g^*) combinations predominantly originate from the atomic p valence shells of each Te atom. Hence, their actual description will be a sensitive measure of an appropriate account of both SC effects and SO coupling.

TABLE IV. SCF total energy (E) and orbital energies of selected doubly degenerate occupied orbitals (ϵ) for Og_2 as obtained from HF/v2z calculations within a scalar-relativistic (SC) four-component Dirac–Coulomb (^{4}DC) as well as a two-component Hamiltonian framework, including the new SC-(e)amfX2C$_{DC}$ models. All energies are given in Hartree.

	SC-1eX2C$_D$	SC-AMFIX2C$_D$	SC-amfX2C$_{DC}$	SC-eamfX2C$_{DC}$	SC-^{4}DC
E	−109 086.488 92	−109 086.488 92	−109 171.759 16	−109 171.759 16	−109 171.759 17
ϵ_{1-2}	−8263.961 72	−8263.961 72	−8291.155 82	−8291.155 82	−8291.155 82
ϵ_{3-4}	−1738.628 22	−1738.628 22	−1743.946 21	−1743.946 21	−1743.946 21
ϵ_{5-10}	−1263.678 16	−1263.678 16	−1264.709 96	−1264.709 96	−1264.709 96
ϵ_{11-12}	−476.535 15	−476.535 15	−477.774 97	−477.774 97	−477.774 97
ϵ_{13-18}	−350.213 16	−350.213 16	−350.499 58	−350.499 58	−350.499 58
$\epsilon_{19-,28}$	−274.235 99	−274.235 99	−274.322 51	−274.322 50	−274.322 50
$\epsilon_{29-,30}$	−142.642 44	−142.642 44	−142.988 85	−142.988 85	−142.988 85
ϵ_{31-36}	−101.557 38	−101.557 38	−101.630 35	−101.630 35	−101.630 35
ϵ_{37-46}	−72.823 70	−72.823 70	−72.836 82	−72.836 82	−72.836 82
ϵ_{47-60}	−48.968 07	−48.968 07	−48.961 63	−48.961 63	−48.961 63
$\cdots$	$\cdots$	$\cdots$	$\cdots$	$\cdots$	$\cdots$
ϵ_{110}	−1.616 33	−1.616 33	−1.614 83	−1.614 82	−1.614 82
ϵ_{111}	−1.311 32	−1.311 32	−1.315 93	−1.315 93	−1.315 93
ϵ_{112}	−1.310 05	−1.310 05	−1.314 67	−1.314 67	−1.314 67
ϵ_{113}	−0.414 45	−0.414 45	−0.414 35	−0.414 35	−0.414 35
ϵ_{114}	−0.396 48	−0.396 48	−0.396 39	−0.396 39	−0.396 39
ϵ_{115}	−0.396 48	−0.396 48	−0.396 39	−0.396 39	−0.396 39
ϵ_{116}	−0.389 81	−0.389 81	−0.389 72	−0.389 72	−0.389 72
ϵ_{117}	−0.389 81	−0.389 81	−0.389 72	−0.389 72	−0.389 72
ϵ_{118}	−0.373 49	−0.373 49	−0.373 41	−0.373 41	−0.373 41

TABLE V. SCF total energy (E) and spinor energies of selected doubly degenerate occupied spinors (ϵ) for Og_2 as obtained from DFT/PBE/v2z calculations within a scalar-relativistic (SC) four-component Dirac–Coulomb (^{4}DC) as well as a two-component Hamiltonian framework, including the new SC-(e)amfX2C$_{DC}$ models. All energies are given in Hartree.

	SC-1eX2C$_D$	SC-AMFIX2C$_D$	SC-amfX2C$_{DC}$	SC-eamfX2C$_{DC}$	SC-^{4}DC
E	−109 137.697 23	−109 137.697 23	−109 230.565 34	−109 230.565 35	−109 230.565 35
ϵ_{1-2}	−8210.621 33	−8210.621 33	−8245.939 22	−8245.939 21	−8245.939 22
ϵ_{3-4}	−1719.076 35	−1719.076 35	−1725.221 40	−1725.221 40	−1725.221 40
ϵ_{5-10}	−1248.586 16	−1248.586 16	−1251.036 14	−1251.036 14	−1251.036 14
ϵ_{11-12}	−466.816 28	−466.816 28	−468.191 09	−468.191 09	−468.191 09
ϵ_{13-18}	−342.387 39	−342.387 39	−342.985 98	−342.985 98	−342.985 98
$\epsilon_{19-,28}$	−267.997 53	−267.997 53	−268.224 50	−268.224 50	−268.224 50
$\epsilon_{29-,30}$	−137.508 75	−137.508 75	−137.878 18	−137.878 17	−137.878 17
ϵ_{31-36}	−97.302 11	−97.302 11	−97.451 28	−97.451 27	−97.451 27
ϵ_{37-46}	−69.594 60	−69.594 60	−69.634 17	−69.634 15	−69.634 15
ϵ_{47-60}	−46.686 30	−46.686 30	−46.682 01	−46.682 00	−46.682 00
$\cdots$	$\cdots$	$\cdots$	$\cdots$	$\cdots$	$\cdots$
ϵ_{110}	−1.297 93	−1.297 93	−1.296 19	−1.296 18	−1.296 18
ϵ_{111}	−1.019 44	−1.019 44	−1.022 82	−1.022 81	−1.022 81
ϵ_{112}	−1.018 77	−1.018 77	−1.022 15	−1.022 15	−1.022 15
ϵ_{113}	−0.281 86	−0.281 86	−0.281 90	−0.281 90	−0.281 90
ϵ_{114}	−0.268 43	−0.268 43	−0.268 51	−0.268 50	−0.268 50
ϵ_{115}	−0.268 43	−0.268 43	−0.268 51	−0.268 50	−0.268 50
ϵ_{116}	−0.263 31	−0.263 31	−0.263 39	−0.263 39	−0.263 39
ϵ_{117}	−0.263 31	−0.263 31	−0.263 39	−0.263 39	−0.263 39
ϵ_{118}	−0.251 40	−0.251 40	−0.251 51	−0.251 50	−0.251 50

To this end, we will not only consider spin-same-orbit but also spin-other-orbit interaction effects where the latter requires the inclusion of the 2e Gaunt term in the many-body Dirac Hamiltonian.[3,93]

In Table VI, we start our assessment of molecular spinor energies of Te_2 obtained by means of AOC-HF calculations by comparing first data based on various 2ePCE corrections schemes for the X2C Hamiltonian to 4c Dirac–Coulomb Hamiltonian reference values. Notably, for the (closed) core electronic shells, we observe for all 2c Hamiltonian schemes, similar trends as was the case for Og_2—with a reference-matching accuracy of our (e)amfX2C models better than 5×10^{-5} Hartree—which underlines the numerical superiority of our newly proposed PCE correction schemes also in an open-shell case. Moving next to the lower end of Table VI, i.e., the (partially) occupied valence π ($\epsilon_{50,-,51}$) and π^* (ϵ_{52-53}) shells, we first note that employing a bare $1eX2C_D$ Hamiltonian does not suffice to achieve sub-mHartree accuracy in the description of the spin–orbit-split m_j components of the $\pi^{(*)}$ shells, in particular for the $\pi^*_{1/2} - \pi^*_{3/2}$ shells (ϵ_{52} and ϵ_{53} in Table VI, respectively). Notably, similar conclusions as for the AOC-HF data in Table VI also hold for the Kramers-unrestricted HF data compiled in Table VII. By contrast—as opposed to the superheavy diatomic Og_2—for the heavy Te_2 diatomic system, the $AMFIX2C_D$ Hamiltonian yields results for the valence shells on par with the (e)amfX2C$_{DC}$ Hamiltonian, both of which are, in turn, in excellent agreement with the ^4DC reference.

We note in passing that the excellent agreement in *absolute* values between $AMFIX2C_D$-based data (encompassing spin-same and spin-other-orbit PCE corrections) and the ^4DCG reference deteriorates not only for the inner-core shells but also for the valence $\pi^{(*)}$ manifolds as shown in Table VIII. More importantly, though, *relative* energy differences are, to a large extent, preserved in the valence shells of Te_2, which suggests that the $AMFIX2C_D$ model could still be a viable option for a 2c Hamiltonian framework when aiming for a study of valence-shell dominated molecular properties. Albeit the reasonable relative energy differences in the latter case, achieving both accurate absolute and relative molecular spinor energies with respect to the ^4DC as well as ^4DCG reference data simultaneously necessitates resorting to our (e)amfX2C Hamiltonian models. As can be inferred from Tables VI and VIII, both our amf 2ePCE correction models display for *all* electronic shells a numerical accuracy within at least a few 10^{-5} Hartree (or better) in comparison to the respective 4c reference.

3. Methane—The ultrarelativistic case

In contrast to the previous molecular examples, methane (CH_4) consists of a "heavy" carbon atom C and four "light" hydrogen atoms H. Particularly, since hydrogen is a *one*-electron system, it will not give rise to atomic *two*-electron PCE correction terms. Hence, any genuine *atomic*-mean-field-based PCE-corrected 2c Hamiltonian, such as $AMFIX2C$ or $amfX2C$, will, by construction, not include any "light"-atom PCE corrections. By contrast, our extended $amfX2C$ approach allows us to eliminate this apparent shortcoming because,

TABLE VI. SCF total energy (E) and spinor energies (ϵ) of the doubly degenerate occupied and (partially occupied) open-shell spinors for Te_2 as obtained from AOC/HF/v2z calculations within a four-component Dirac–Coulomb (^4DC) as well as a two-component Hamiltonian framework, including the new (e)amfX2C$_{DC}$ models. All energies are given in Hartree.

	$1eX2C_D$	$AMFIX2C_D$	$amfX2C_{DC}$	$eamfX2C_{DC}$	^4DC
E	−13 584.541 93	−13 584.340 21	−13 587.741 21	−13 587.741 19	−13 587.741 74
ϵ_{1-2}	−1174.973 31	−1174.977 84	−1176.015 76	−1176.015 76	−1176.015 72
ϵ_{3-4}	−183.754 95	−183.756 45	−183.876 40	−183.876 40	−183.876 40
ϵ_{5-6}	−172.035 41	−171.693 23	−171.763 85	−171.763 85	−171.763 85
ϵ_{7-8}	−161.416 35	−161.570 69	−161.637 31	−161.637 30	−161.637 31
$\epsilon_{9,-,10}$	−161.416 20	−161.570 54	−161.637 16	−161.637 16	−161.637 16
ϵ_{11-12}	−38.108 99	−38.109 52	−38.130 87	−38.130 86	−38.130 86
ϵ_{13-14}	−33.171 92	−33.102 76	−33.113 02	−33.113 02	−33.113 02
ϵ_{15-16}	−31.132 06	−31.163 70	−31.173 36	−31.173 35	−31.173 35
ϵ_{17-18}	−31.130 92	−31.162 56	−31.172 22	−31.172 22	−31.172 22
$\epsilon_{19,-,20}$	−22.491 55	−22.431 46	−22.432 28	−22.432 28	−22.432 28
ϵ_{21-22}	−22.489 93	−22.429 84	−22.430 65	−22.430 65	−22.430 65
ϵ_{23-24}	−21.991 04	−22.030 63	−22.032 48	−22.032 47	−22.032 47
ϵ_{25-26}	−21.990 31	−22.029 90	−22.031 75	−22.031 74	−22.031 74
ϵ_{27-28}	−21.988 93	−22.028 52	−22.030 37	−22.030 38	−22.030 38
$\cdots$	$\cdots$	$\cdots$	$\cdots$	$\cdots$	$\cdots$
ϵ_{47}	−0.865 60	−0.865 65	−0.865 90	−0.865 90	−0.865 90
ϵ_{48}	−0.703 08	−0.703 12	−0.703 48	−0.703 47	−0.703 47
ϵ_{49}	−0.414 23	−0.413 90	−0.413 89	−0.413 89	−0.413 89
ϵ_{50}	−0.365 88	−0.365 17	−0.365 14	−0.365 13	−0.365 13
ϵ_{51}	−0.343 37	−0.343 89	−0.343 86	−0.343 87	−0.343 87
ϵ_{52}	−0.260 21	−0.259 90	−0.259 90	−0.259 90	−0.259 90
ϵ_{53}	−0.239 43	−0.240 03	−0.240 03	−0.240 03	−0.240 03

TABLE VII. SCF total energy (E) and spinor energies (ϵ) of occupied spinors for Te$_2$ as obtained from Kramers-unrestricted HF/v2z calculations within a four-component Dirac–Coulomb (^{4}DC) as well as a two-component Hamiltonian framework, including the new (e)amfX2C$_{DC}$ models. All energies are given in Hartree.

	1eX2C$_D$	amfX2C$_{DC}$	eamfX2C$_{DC}$	^{4}DC
E	−13 584.660 07	−13 587.858 59	−13 587.858 62	−13 587.859 37
ϵ_{1-2}	−1174.972 17	−1176.014 50	−1176.014 50	−1176.014 66
	−1174.969 88	−1176.012 19	−1176.012 19	−1176.012 43
ϵ_{3-4}	−183.752 81	−183.874 41	−183.874 41	−183.874 42
	−183.752 00	−183.873 60	−183.873 60	−183.873 62
ϵ_{5-6}	−172.033 33	−171.761 93	−171.761 92	−171.761 92
	−172.033 07	−171.761 67	−171.761 66	−171.761 67
ϵ_{7-8}	−161.414 72	−161.635 82	−161.635 81	−161.635 82
	−161.414 62	−161.635 72	−161.635 71	−161.635 72
$\epsilon_{9,-,10}$	−161.412 62	−161.633 73	−161.633 73	−161.633 76
	−161.412 59	−161.633 70	−161.633 70	−161.633 73
ϵ_{11-12}	−38.107 49	−38.129 53	−38.129 53	−38.129 53
	−38.104 95	−38.126 98	−38.126 98	−38.126 98
ϵ_{13-14}	−33.169 88	−33.111 13	−33.111 13	−33.111 13
	−33.169 37	−33.110 64	−33.110 63	−33.110 64
ϵ_{15-16}	−31.130 53	−31.171 99	−31.171 99	−31.171 99
	−31.130 50	−31.171 95	−31.171 95	−31.171 95
ϵ_{17-18}	−31.126 56	−31.168 03	−31.168 03	−31.168 04
	−31.126 52	−31.168 00	−31.168 00	−31.168 00
$\epsilon_{19,-,20}$	−22.488 91	−22.429 80	−22.429 80	−22.429 80
	−22.488 70	−22.429 58	−22.429 58	−22.429 58
ϵ_{21-22}	−22.487 51	−22.428 39	−22.428 38	−22.428 39
	−22.487 48	−22.428 36	−22.428 35	−22.428 36
ϵ_{23-24}	−21.988 41	−22.030 01	−22.030 00	−22.030 01
	−21.988 19	−22.029 79	−22.029 78	−22.029 78
. . .	. . .	. . .	. . .	. . .
ϵ_{99}	−0.418 95	−0.418 81	−0.418 81	−0.418 80
ϵ_{100}	−0.397 75	−0.397 42	−0.397 42	−0.397 42
ϵ_{101}	−0.323 64	−0.323 79	−0.323 79	−0.323 79
ϵ_{102}	−0.321 15	−0.321 51	−0.321 51	−0.321 51
ϵ_{103}	−0.317 81	−0.317 69	−0.317 69	−0.317 69
ϵ_{104}	−0.315 21	−0.315 27	−0.315 28	−0.315 28

as detailed in Sec. II C and outlined in lines 14–23 of Algorithm 2, all PCE correction terms for HF and DFT, respectively, are derived in *molecular* basis on the basis of molecular densities, $D_\oplus^{4c}$ and $D_\oplus^{2c}$, built from a superposition of atomic input densities. Consequently, the essential molecular densities include atomic contributions regardless of the actual atom type, that is, both "light" (one-electron) and "heavy" (many-electron) atoms contribute equally.

Bearing the latter in mind, the total SCF energies as well as spinor energies compiled in Table IX for an ultrarelativistic CH$_4$ with the speed of light c scaled down by a factor 10 confirm the unique numerical performance of the eamfX2C$_{DC}$ Hamiltonian model in comparison to the ^{4}DC reference data. Only in the eamfX2C$_{DC}$ case (column four, Table IX), we find that not only the total energy E agrees to better than mHartree accuracy but also the spinor energies exhibit consistent numerical accuracy for the innermost non-bonding core C 1s as well as the bonding, valence C–H spinors. Notably, the amfX2C$_{DC}$ and the AMFIX2C$_D$

models feature an inconsistent numerical performance with respect to both quantities: amfX2C$_{DC}$ yields a total energy E and spinor energies for the (carbon-centered) inner-core spinors ϵ_1 and ϵ_2, respectively, of the ultrarelativistic CH$_4$, which are in close agreement with the ^{4}DC reference. It shows, however, larger deviations for the valence spinors (ϵ_{3-5}) whereas the opposite conclusions apply to the AMFIX2C$_D$-based data. In the latter case, we ascribe the seemingly good performance of the AMFIX2C$_D$ Hamiltonian with errors less than a mHartree in comparison to the ^{4}DC reference to a fortuitous error cancellation since the amf-based AMFI PCE correction scheme cannot take into account any 2e picture-change correction that involves contributions from the atomic hydrogen centers.

B. Contact densities of copernicium fluorides CnF$_n$

In this section, we assess the accuracy of calculating absolute contact densities as well as the potential to provide reliable relative

TABLE VIII. SCF total energy (E) and spinor energies (ϵ) of the doubly degenerate occupied and open-shell spinors for Te$_2$ as obtained from AOC/HF/v2z calculations within a four-component Dirac–Coulomb–Gaunt (^{4}DCG) as well as a two-component Hamiltonian framework, including the new (e)amfX2C$_{DCG}$ models. All energies are given in Hartree.

	1eX2C$_D$	AMFIX2C$_D$	amfX2C$_{DCG}$	eamfX2C$_{DCG}$	^{4}DCG
E	−13 584.541 93	−13 584.254 57	−13 576.460 87	−13 576.460 83	−13 576.457 40
ϵ_{1-2}	−1174.973 31	−1174.980 60	−1173.197 96	−1173.197 96	−1173.197 89
ϵ_{3-4}	−183.754 95	−183.757 37	−183.615 71	−183.615 71	−183.615 70
ϵ_{5-6}	−172.035 41	−171.613 03	−171.294 09	−171.294 09	−171.294 08
ϵ_{7-8}	−161.416 35	−161.603 82	−161.302 79	−161.302 79	−161.302 80
$\epsilon_{9,-,10}$	−161.416 20	−161.603 66	−161.302 63	−161.302 64	−161.302 63
ϵ_{11-12}	−38.108 99	−38.109 82	−38.094 68	−38.094 68	−38.094 68
ϵ_{13-14}	−33.171 92	−33.086 83	−33.041 33	−33.041 33	−33.041 33
ϵ_{15-16}	−31.132 06	−31.170 31	−31.127 09	−31.127 08	−31.127 09
ϵ_{17-18}	−31.130 92	−31.169 16	−31.125 94	−31.125 95	−31.125 95
$\epsilon_{19,-,20}$	−22.491 55	−22.425 20	−22.412 06	−22.412 06	−22.412 06
ϵ_{21-22}	−22.489 93	−22.423 58	−22.410 44	−22.410 44	−22.410 44
ϵ_{23-24}	−21.991 04	−22.035 03	−22.023 48	−22.023 47	−22.023 47
ϵ_{25-26}	−21.990 31	−22.034 30	−22.022 75	−22.022 75	−22.022 75
ϵ_{27-28}	−21.988 93	−22.032 93	−22.021 38	−22.021 39	−22.021 39
. . .	. . .	. . .	. . .	. . .	. . .
ϵ_{47}	−0.865 60	−0.865 67	−0.865 83	−0.865 82	−0.865 82
ϵ_{48}	−0.703 08	−0.703 13	−0.703 23	−0.703 22	−0.703 22
ϵ_{49}	−0.414 23	−0.413 82	−0.413 60	−0.413 59	−0.413 60
ϵ_{50}	−0.365 88	−0.365 01	−0.364 80	−0.364 79	−0.364 79
ϵ_{51}	−0.343 37	−0.344 00	−0.343 82	−0.343 83	−0.343 83
ϵ_{52}	−0.260 21	−0.259 83	−0.259 52	−0.259 53	−0.259 53
ϵ_{53}	−0.239 43	−0.240 16	−0.239 87	−0.239 87	−0.239 87

contact density shifts computed within PCE-corrected X2C Hamiltonian models by comparing to parent 4c reference data. While absolute contact densities are dominated by contributions of the inner s-shells, and to a lesser extent the innermost $p_{1/2}$-shells, of the respective nuclear center of interest, contact density shifts particularly probe subtle differences of the valence electronic structure and, likewise, polarization of the inner electronic shells, both of which originate from the chemical bonding between a reference atom, here the Cn atom, and ligand atoms (or molecules), as for example, the n fluorine atoms in the CnF$_n$ compounds studied in the present work. The optimized structures of the CnF$_n$ ($n = 2, 4, 6$) compounds along with the corresponding spatial symmetries are shown in Table X.

Considering the limited basis-set size and point nucleus approximation in the present work, our optimized Cn–F bond lengths $r_{Cn–F}$ compare reasonably with corresponding benchmark data from a very recent work by Hu and Zou[85] who reported X2C/PBE0-optimized bond lengths $r_{Cn–F}$ of 1.920, 1.927, and 1.933 Å with an increasing number n of fluorine ligand atoms.

Table XI summarizes the calculated absolute contact densities as well as density shifts in a spin-dependent (upper panel) and scalar-relativistic (spinfree, lower panel) framework. As can be seen there, by construction, we find for the bare Cn atom to be a perfect match for the absolute contact density at the Cn nucleus between our (e)amfX2C$_{DC}$ PCE-corrected 2c calculations (Table XI, entries 4

TABLE IX. SCF total energy (E) and spinor energies (ϵ) of the doubly degenerate occupied spinors for CH$_4$ as obtained from DFT/PBE/v2z calculations within a four-component Dirac–Coulomb (^{4}DC) as well as a two-component Hamiltonian framework, including the new (e)amfX2C$_{DC}$ models. All energies are given in Hartree. The speed of light c was reduced by a factor 10.

	1eX2C$_D$	AMFIX2C$_D$	amfX2C$_{DC}$	eamfX2C$_{DC}$	^{4}DC
E	−42.142 20	−42.140 39	−42.264 69	−42.257 74	−42.258 50
ϵ_1	−10.222 06	−10.224 01	−10.361 54	−10.360 28	−10.357 94
ϵ_2	−0.659 39	−0.659 66	−0.662 88	−0.662 69	−0.662 74
ϵ_3	−0.357 05	−0.352 88	−0.356 49	−0.352 91	−0.352 90
ϵ_{4-5}	−0.333 13	−0.335 03	−0.332 82	−0.335 27	−0.335 44

TABLE X. Four-component DFT/PBE0-optimized structures of CnF_n ($n = 2, 4, 6$) compounds. For computational details, see text. All internuclear distances r_{Cn-F} are given in Å.

Molecule	r_{Cn-F}	Double group symmetry
CnF_2	1.937	$D_{\infty h}^*$
CnF_4	1.942	C_{4h}^*
CnF_6	1.948	O_h^*

and 5) and the corresponding 4c reference, irrespective of the inclusion of spin-dependent terms. By contrast, discarding any 2ePCE correction (1eX2C$_D$, entry 2) or including only first-order SO mean-field PCE corrections (AMFIX2C$_D$, entry 3) leads to a considerable underestimation of the total contact density. Interestingly, in the AMFIX2C$_D$ case, the total contact density is even smaller than in the 1eX2C$_D$ case and, consequently, in even stronger disagreement with the 4c reference. Moving next to the difluoride compound, the conclusions surprisingly seem to shift. While all 2c models correctly reproduce the trend of a decrease in the contact density at the Cn nucleus, AMFIX2C$_D$ (923.43 e/a_0^3, spinfree: 1225.51 e/a_0^3) now exhibits the best agreement for the contact density shift with the (sc-)^{4}DC reference of 922.84 e/a_0^3 (1226.40 e/a_0^3). Considering the remaining tetra- and hexafluoride compounds in Table XI, the agreement of AMFIX2C$_D$ for $\Delta\rho$ with the 4c references considerably worsens with an increasing number of fluorine ligands. This leads us to conclude that the almost perfect match in $\Delta\rho$ observed for CnF_2 is likely due to a fortuitous error cancellation.

What about the (e)amfX2C models? For CnF_2, a decomposition of the total contact density at the Cn nucleus in terms of molecular spinor contributions reveals that calculations based on the (e)amfX2C$_{DC}$ Hamiltonian predict in the spin-dependent case—with similar conclusions holding for the spinfree case—a major contribution of the Cn 1s shell (*vide supra*) of $-43\,605\,705.12$ e/a_0^3 ($-43\,605\,705.33$ e/a_0^3) in contrast to the 4c value of $-43\,605\,699.65$ e/a_0^3. Hence, recalling the exact numerical match within significant digits for the bare Cn atom (see Table XI, first row), the major source for the difference in the total $\Delta\rho$ for CnF_2 predominantly traces back to a $\Delta\rho_{1s} \approx 5.5$ e/a_0^3 between our 2c (e)amfX2C$_{DC}$ and the ^{4}DC data. Moreover, it is precisely for this innermost electronic shell that the molecular spinor energies ϵ_{1s} exhibit deviations between (e)amfX2C and ^{4}DC on the order of $+3 \times 10^{-4}$ Hartree. In detail, we obtain in both 2c cases $\epsilon_{1s}^{amfX2C_{DC}} = -7117.032\,93$, Hartree and $\epsilon_{1s}^{eamfX2C_{DC}} = -7117.032\,94$ Hartree, respectively, underlining the obvious close relationship of the two approaches, which have to be compared with $\epsilon_{1s}^{^4DC} = -7117.032\,60$ Hartree. Despite the slightly increasing discrepancies in $\Delta\rho$ observed for the remaining polyatomic fluoride compounds of Cn listed in Table XI, which can be explained along the same lines as for the difluoride CnF_2 compound, our (e)amfX2C models still perform best in a systematic fashion with respect to the four-component references. Notably, these encouraging findings hold for both common-use cases, with the inclusion of SO interaction and in a genuine spinfree approach. In summary, probing the density at a heavy nucleus constitutes an excellent measure of the importance of 2e interaction contributions and, hence, allows us to uniquely reveal even subtle shortcomings of distinct 2ePCE correction models within the X2C Hamiltonian framework by comparing to the corresponding full 4c reference data.

C. X-ray core-ionization energies

Finally, we compare the performance and reliability of the 1eX2C, AMFIX2C as well as (e)amfX2C 2c Hamiltonian models

TABLE XI. Contact densities ρ and contact density shifts $\Delta\rho$ evaluated at the Cn nucleus for the Cn atom and different Cn fluoride compounds. All data were obtained from scalar-relativistic + spin–orbit (upper panel) and scalar-relativistic-only spinfree (lower panel) HF wave functions. For the two-component X2C Hamiltonian, different two-electron picture-change effect corrections were employed, including the new (e)amfX2C$_{DC}$ models. All densities are given in e/a_0^3.

Compound	1eX2C$_D$	AMFIX2C$_D$	amfX2C$_{DC}$	eamfX2C$_{DC}$	^{4}DC
Cn	$-58\,697\,556.08$	$-58\,661\,390.26$	$-58\,977\,494.39$	$-58\,977\,494.39$	$-58\,977\,494.39$
CnF_2	$-58\,696\,660.51$	$-58\,660\,466.83$	$-58\,976\,578.21$	$-58\,976\,577.94$	$-58\,976\,571.54$
CnF_4	$-58\,695\,900.03$	$-58\,659\,721.50$	$-58\,975\,824.80$	$-58\,975\,823.87$	$-589\,75\,812.06$
CnF_6	$-586\,95\,683.21$	$-58\,659\,514.86$	$-58\,975\,609.89$	$-58\,975\,608.50$	$-589\,75\,593.75$
$\Delta\rho_{(CnF_2-Cn)}$	895.57	923.43	916.18	916.45	922.84
$\Delta\rho_{(CnF_4-Cn)}$	1656.05	1668.76	1669.58	1670.52	1682.33
$\Delta\rho_{(CnF_6-Cn)}$	1872.88	1875.40	1884.50	1885.89	1900.64
Spinfree					
Cn	$-56\,251\,080.53$	$-56\,251\,080.53$	$-56\,571\,626.66$	$-56\,571\,626.66$	$-565\,71\,626.66$
CnF_2	$-56\,249\,855.02$	$-56\,249\,855.02$	$-56\,570\,406.42$	$-56\,570\,405.90$	$-56\,570\,400.26$
CnF_4	$-56\,249\,040.54$	$-56\,249\,040.54$	$-56\,569\,579.69$	$-56\,569\,578.93$	$-56\,569\,569.39$
CnF_6	$-56\,248\,766.28$	$-56\,248\,766.28$	$-56\,569\,295.28$	$-56\,569\,294.35$	$-56\,569\,283.33$
$\Delta\rho_{(CnF_2-Cn)}$	1225.51	1225.51	1219.24	1220.79	1226.40
$\Delta\rho_{(CnF_4-Cn)}$	2039.99	2039.99	2046.97	2047.73	2057.27
$\Delta\rho_{(CnF_6-Cn)}$	2314.25	2314.25	2331.38	2332.31	2343.33

for the calculation of x-ray core-ionization energies by comparing to corresponding mmfX2C reference values. With the advent and general accessibility of new, powerful x-ray radiation sources, such as free-electron lasers[94] (see, for example, Ref. 95 for an overview of available facilities), experimental x-ray spectroscopy has witnessed in the past decade a continuous, rapid advance and enhanced applicability to study not only the electronic structure but also the dynamics of molecules and materials.[96–98] In order to keep pace with the experimental progress and be able to provide a much welcomed highly accurate theoretical support, computational x-ray spectroscopy has experienced tremendous progress in recent years.[99] Here, a genuine inclusion of relativistic effects is nothing but a basic requirement since the inner-core shells are most prone to quantitative changes due to relativity. For example, while K-edge x-ray spectroscopy probes the chemical nature of the $1s_{1/2}$ shell of a given center and, hence, necessitates, in particular, a proper account of SC contributions, studying the L-edge and M-edge of (late) transition-metal, p-block and, perhaps most importantly, f-elements,[100] whose fine-structure is dominated by the SO splitting of the $2p$- and $3p$- and $3d$-shells, respectively, requires a suitable framework to efficiently take into account the SO interaction. The latter two requirements are easily met in either a (exact) 2c or full 4c framework that sets out from a many-particle Dirac–Coulomb(–Gaunt/Breit) Hamiltonian. For further details and recent advances of genuine relativistic quantum-chemical x-ray spectroscopy approaches that illustrate in a striking fashion the potential of such ansätze, we refer the reader, for example, to Refs. 89 and 101–104.

Considering common applications in x-ray spectroscopy, we highlight in Table XII and XIII the importance of 2ePCE corrections to the X2C Hamiltonian, which we may anticipate, based on all findings discussed in the previous sections (*vide supra*), to be most pronounced for the K- up to M-edges of heavy- and superheavy nuclei. Starting with the EOM-CCSD core-ionization potentials of the heavy p-block anion At^- compiled in Table XII, we note that the K-edge ionization potentials within both the 1eX2C$_D$ and AMFIX2C$_D$ Hamiltonian frameworks deviate more than 5 Hartree (sic!) from the mmfX2C$_{DC}$ reference. Concerning the use of the latter, it was shown in Ref. 89 that making use of this 2c Hamiltonian scheme yields ionization potentials that are virtually indistinguishable from the parent ^{4}DC data and this is indeed confirmed by the present calculations. Moving to our (e)amfX2C PCE-corrected Hamiltonian framework, we observe an agreement with the mmfX2C$_{DC}$ data of sub-mHartree accuracy not only for the K-edge but also for the L$_1$-

as well as L$_{2,3}$-edges. The resulting deviation of 47 cm^{-1} from the reference data for the SO splitting Δ_{L-edge}^{SO} (fifth row, Table XII), which ultimately governs the fine-structure of the L$_{2,3}$-edges, approaches almost *spectroscopic* accuracy of 1 cm^{-1}.[105] By contrast, the error for Δ_{L-edge}^{SO} in the case of employing, for example, the hitherto popular AMFIX2C$_D$ Hamiltonian is as large as 21 600 cm^{-1} (corresponding to an error that is 60 times (sic!) larger than the error bar for *chemical* accuracy).

Table XIII compiles core-ionization potential data for two representative molecular $5d$ (upper panel) and $6d$ (lower panel) complexes as obtained from EOM-CCSD calculations. As was the case for the At^- anion, we consider the numerical performance of different *atomic* mean-field 2ePCE-correction schemes for the X2C Hamiltonian by comparing to results calculated within a *molecular* mean-field 2c framework (Table XIII, entry 6). In passing, we note that for the [Au]-complex (upper panel of Table XIII), we were not able to obtain a converged SCF solution for Au within the external SCF program RELSCF[106] that constitutes the basis for the AMFI module within DIRAC, and this is unfortunately a recurring problem. Considering first the full neglect of 2ePCE corrections within the 1eX2C$_D$ framework (Table XIII, entry 2), a similar picture emerges in both molecular cases as in the single-ion case. The absolute deviations for the ionization potentials of all K- to M-edges are substantial. Moreover, the same conclusions hold for relative deviations, exemplified by the SO splittings Δ_{L-edge}^{SO} of the L-edge. Hence, these findings unequivocally demonstrate also in the context of x-ray spectroscopic quantities that 2ePCEs are substantial when probing molecular properties of the inner-core shells. Interestingly, though, the ligand-field induced splittings of the M$_{4,5}$-edges in the case of the [Au]-complex can be correctly reproduced within the 1eX2C$_D$ Hamiltonian framework. As can be seen for the CnF$_2$ complex, the inclusion of first-order mean-field SO PCE corrections (entry 3, Table XIII) within the AMFIX2C$_D$ Hamiltonian leads to a reduction of the error for Δ_{L-edge}^{SO} by one order of magnitude from $\Delta\Delta_{L-edge}^{SO} \approx +8.7$ Hartree (1eX2C$_D$) to $\Delta\Delta_{L-edge}^{SO} \approx -0.7$ Hartree. Still, the underlying absolute core-ionization potentials for the K- and L-edges exhibit a clear deviation ranging from ~1.2 Hartree for the L$_3$-edge to more than 17 Hartree for the K-edge in comparison to the mmfX2C$_{DC}$ data.

By contrast, the EOM-CCSD core-ionization potentials calculated within the (e)amfX2C$_{DC}$ Hamiltonian frameworks (entries 4 and 5 in Table XIII) stand out also in the molecular cases due to

TABLE XII. EOM-CCSD/dyall.acv3z core-ionization energies of the At^- anion obtained within a two-component Hamiltonian framework employing different corrections for two-electron picture-change effects. Note that for At^- amfX2C$_{DC}$ and eamfX2C$_{DC}$ yield identical results. All energies are given in Hartree.

Ionization	1eX2C$_D$	AMFIX2C$_D$	amfX2C$_{DC}$	amfX2C$_{DC}$[a]	mmfX2C$_{DC}$[b]
K-edge	3532.8949	3532.9393	3538.2640	3538.2642	3538.2639
L$_1$-edge	644.5913	644.6059	645.4290	645.4290	645.4290
L$_2$-edge	620.8625	618.7619	619.2730	619.2730	619.2728
L$_3$-edge	522.5137	523.2968	523.7092	523.7092	523.7092
Δ_L^{SO}	98.3488	95.4651	95.5638	95.5638	95.5636

[a]amf corrections calculated for a neutral at atom.
[b]mmfX2C$_{DC} \equiv$ ^{2}DC^m values taken from Ref. 89.

TABLE XIII. EOM-CCSD/v2z core-ionization energies of the molecular compounds $[Au(Cl)_4]^-$ and CnF_6 obtained within a two-component Hamiltonian framework employing different corrections for two-electron picture-change effects, including the new (e)amfX2C$_{DC}$ models. All energies are given in Hartree.

Ionization	1eX2C$_D$	AMFIX2C$_D$	amfX2C$_{DC}$	eamfX2C$_{DC}$	mmfX2C$_{DC}$	^{4}DC
			$[AuCl_4]^-$			
K-edge	2982.8305	n/a	2986.9702	2986.9702	2986.9702	2986.9705
L$_1$-edge	531.1267	n/a	531.7386	531.7387	531.7386	531.7387
L$_2$-edge	509.7823	n/a	508.5810	508.5810	508.5809	508.5808
L$_3$-edge	440.0794	n/a	441.0060	441.0061	441.0060	441.0064
	440.0792	n/a	441.0058	441.0058	441.0058	441.0061
M$_4$-edge	85.6431	n/a	85.3486	85.3487	85.3486	85.3485
	85.6414	n/a	85.3471	85.3471	85.3471	85.3470
M$_5$-edge	81.9117	n/a	82.1323	82.1323	82.1322	82.1325
	81.9097	n/a	82.1302	82.1303	82.1302	82.1305
	81.9082	n/a	82.1290	82.1290	82.1290	82.1292
$^a\Delta^{SO}_{L-edge}$	69.7030	n/a	67.5751	67.5751	67.5750	67.5745
$\Delta\Delta^{SO}_{L-edge}$	2.1280	n/a	0.0001	0.0001	0	$\cdots$
			CnF_6			
K-edge	7098.8642	7099.0856	7116.4597	7116.4597	7116.4590	7116.4585
L$_1$-edge	1450.8351	1450.9066	1454.3983	1454.3984	1454.3979	1454.3983
L$_2$-edge	1412.3308	1404.9511	1406.9201	1406.9201	1406.9198	1406.9194
L$_3$-edge	1003.1544	1005.1986	1006.4395	1006.4396	1006.4393	1006.4401
Δ^{SO}_{L-edge}	409.1763	399.7525	400.4806	400.4806	400.4804	400.4793
$\Delta\Delta^{SO}_{L-edge}$	8.6959	−0.7279	0.0002	0.0002	0	$\cdots$

^{a}Calculated as $\Delta^{SO}(L_2$-$\bar{L}_3)$ using an arithmetic mean value for the L$_3$-edge.

two distinct, appealing features: (i) the *absolute* ionization energies for all edges feature numerical values below sub-mHartree accuracy; (ii) as a result, this accuracy carries over to relative data such as the SO splitting of the L$_{2,3}$-edge and the ligand-field fine-structure splitting of the M$_{4,5}$-edges in the [Au]-complex. Hence, the atomic-mean-field (e)amfX2C Hamiltonian models can be regarded as a conceptually different alternative to the molecular mean-field ^{2}DC scheme by providing virtually the same numerical accuracy for core- and likewise valence molecular properties at a fraction of the computational effort. To stress the latter, we recall that the mmfX2C$_{DC}$ approach requires to first find a converged *molecular* 4c SCF solution whereas our (e)amfX2C models are solely built on quantities obtained from *atomic* 4c SCF calculations. In the latter case, the SCF step is then carried out exclusively in a molecular 2c framework. Moreover, we note that, although the extended amfX2C Hamiltonian model requires the calculation of a single 2e Fock matrix $\boldsymbol{F}^{4c,2e}[\boldsymbol{D}^{4c}_\oplus]$ in a molecular four-component framework, an efficient density-matrix-based screening will significantly reduce the associated computational cost because of the sparsity of the atom-wise blocked 4c molecular density matrix $\boldsymbol{D}^{4c}_\oplus$.

Besides the calculation of core binding energies within a 2c Hamiltonian framework taking into account various PCE correction models, we performed ^{4}DC-based EOM-CCSD calculation for the [Au]-complex as well as CnF$_6$ (Table XIII, entry 7). This enables us to further assess the influence of the Hamiltonian on the core ionizations, in particular inherent PCEs in the electron–electron

interaction within a two-component X2C framework, regardless of an mmf or amf model to account for PCEs. As discussed in detail by Halbert *et al.* in Ref. 89 in the context of x-ray core binding energies, even for mmfX2C$_{DC}$, which is based on the transformation
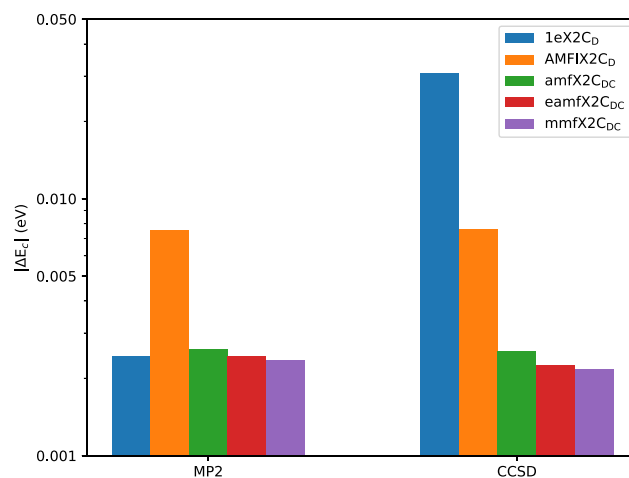
FIG. 2. Absolute MP2 and CCSD correlation energy differences between ^{4}DC ($|\Delta E_c|$, in eV), for different Hamiltonians calculated for CnF$_6$ with the same computational setup as for the EOM-CCSD core-ionization energies. Note that the scale on the y axis is logarithmic. Further computational details are given in the text.

TABLE XIV. EOM-CCSD/v2z core-ionization energies of CnF_6 including contributions from the two-electron Gaunt interaction obtained within a two-component Hamiltonian framework employing different corrections for two-electron picture-change effects, including the new (e)amfX2C$_{DCG}$ models. All energies are given in Hartree.

Ionization	1eX2C$_D$	AMFIX2C$_D$	amfX2C$_{DCG}$	eamfX2C$_{DCG}$	mmfX2C$_{DCG}$
K-edge	7098.864 222 757 124	7099.244 902 278 329	7076.503 732 188 685	7076.503 830 421 792	7076.501 403 453 378
L$_1$-edge	1450.835 145 507 292	1450.960 331 295 658	1448.800 870 735 362	1448.800 972 562 912	1448.800 310 220 434
L$_2$-edge	1412.330 779 914 150	1402.780 910 028 746	1397.811 070 079 591	1397.811 170 997 760	1397.810 400 069 455
L$_3$-edge	1003.154 441 459 877	1005.551 885 385 839	1001.540 331 728 849	1001.540 433 936 657	1001.540 508 582 275
$\Delta_{\text{L-edge}}^{\text{SO}}$	409.176 338 454 273 04	397.229 024 642 906 9	396.270 738 350 742	396.270 737 061 103	396.269 891 487 179 96
$\Delta\Delta_{\text{L-edge}}^{\text{SO}}$	12.906 446 967 093 075	0.959 133 155 726 931 4	0.000 846 863 562 060 207 2	0.000 845 573 923 015 763 3	0

into a 2c framework with respect to a decoupling of the (converged) Fock matrix, leaving the 2e operator untransformed[32] necessarily introduces a PCE in the electron–electron interaction. Hence, the latter becomes most prominent for molecular properties that necessitate an accurate treatment of core–core and core–valence electron correlation such as x-ray core-ionization potentials. Consequently, albeit our limited correlation treatment in the EOM-CCSD step (see Sec. III for further details), we already find small discrepancies for the K- and L-edge ionization energies between mmfX2C$_{DC}$ and ^{4}DC on the order of 0.0025 eV and, similarly, for (e)amfX2C and ^{4}DC with differences up to 0.0035 eV in the case of CnF_6 while the deviations in the binding energies for the corresponding edges are smaller for the [Au]-complex because of the "lighter" Au central atom. As larger deviations—though still less than 0.01% of the total K-edge binding energy—had been observed in a corresponding comparison for astatine,[89] we expect also for CnF_6 (and, similarly, for the [Au]-complex) a further increase of the deviations between ^{4}DC and (e)amfX2C$_{DC}$ as well as mmfX2C$_{DC}$ upon an improved electron correlation treatment. In passing, we note, though, the excellent performance of our extended amfX2C-based computational model (red error bars in Fig. 2) with respect to the mmfX2C$_{DC}$ model (purple error bars in Fig. 2), which are nearly identical for both MP2 and CCSD correlation energies even on a logarithmic scale in the case of CnF_6. By contrast, turning to 1eX2C$_D$ and AMFIX2C$_D$, respectively, we either find stark differences in the correlation errors between the MP2 and CCSD approaches (1eX2C$_D$) or, even within this limited correlation space, considerable errors in the correlation energies within AMFIX2C$_D$ by comparison to the ones obtained within a ^{4}DC framework. Taking together, these findings yet again underline the suitability and superiority of our amfX2C Hamiltonian models, in particular its extended variant, in the realm of an X2C framework for studying x-ray core binding energies of atoms and molecules comprising heavy and superheavy elements.

Finally, Table XIV compiles x-ray EOM-CSCD core binding energies of CnF_6 with the inclusion of the 2e Gaunt interaction. This allows us to highlight the significance of the Gaunt interaction (as part of the full Breit interaction) for an accurate description of the inner-core edges of (super)heavy elements by comparing to the corresponding Coulomb-type-interaction only data shown above in Table XIII. Note that we do not have ^{4}DCG data at hand since the transformation of Gaunt-type AO integrals to MO basis is currently implemented neither in DIRAC nor in RESPECT. In addition, as

discussed for Te_2 in Sec. IV A 2, 1eX2C$_D$ does not allow to take into account contributions from the Gaunt interaction and will not be considered further below.

In agreement with what has been concluded in Ref. 89 for astatide, we find for the (e)amfX2C$_{DCG}$ as well as mmfX2C$_{DCG}$ models (Table XIV, entries 4–6) a distinct effect arising from the Gaunt interaction. As a result, core binding energies are substantially lowered by nearly 40 Hartree [≈ 1.1 keV (!)] in the case of the K-edge and by up to 9 Hartree for the L-edge, respectively. Moreover, we also observe a considerable decrease in the SO splitting of the L$_{2,3}$-edge $\Delta_{\text{L-edge}}^{\text{SO}}$ by ~115 eV, which is very well captured ($\Delta\Delta_{\text{L-edge}}^{\text{SO}} \approx 0.02$ eV) by our (e)amfX2C$_{DCG}$ models in comparison to mmfX2C$_{DCG}$. The latter is in sharp contrast to the AMFIX2C$_D$ model (entry 3), which not only exhibits significant numerical differences in terms of absolute core binding energies of more than 600 eV for the K-edge but also shows a quantitative error $\Delta\Delta_{\text{L-edge}}^{\text{SO}}$ of more than 25 eV for the L$_{2,3}$-edge fine-structure splitting.

V. CONCLUSIONS AND OUTLOOK

In this article, we have presented the motivation for and derivation of two distinct, atomic-mean-field (amf) approaches to account on an equal footing for two-electron (2e) scalar-relativistic and spin–orbit picture-change effects (PCEs) arising within an exact-two-component (X2C) Hamiltonian framework. Both approaches, dubbed amfX2C and extended amf (eamfX2C), have been implemented independently in the DIRAC[5] and RESPECT[6] programs. These implementations, which exploit—where available—atomic supersymmetry in the atomic self-consistent field steps,[5] open up possibilities for the calculation of two-electron picture-change effect corrections for all spin-dependent and spinfree four-component-based Hamiltonians available in the two quantum-chemical software packages.

Notably, we have shown that it is possible to uniquely tailor our amf 2ePCE corrections for the X2C Hamiltonian to the underlying classes of self-consistent field (SCF) *ansätze*: Hartree–Fock (HF) or density functional theory (DFT). Such a particular feature has, to the best of our knowledge, so far not been considered for any 2ePCE correction scheme in the literature. Moreover, by contrast to, for example, the recently proposed SOX2CAMF model,[34] our new PCE correction schemes for the X2C Hamiltonian take

into account both *spin-independent*—that is, scalar-relativistic—and *spin-dependent*—that is, spin–spin (arising from the Gaunt term[93]) as well as spin–orbit—contributions of the two-electron interaction. Perhaps most importantly, we also argue why the eamfX2C Hamiltonian can be employed in genuine two-component solid-state SCF calculations under consideration of periodic boundary conditions starting from an appropriate four-component framework.[107] The latter is subject of ongoing work in our laboratories.

The novel (e)amfX2C models are readily available for genuine two-component atomic and molecular SCF calculations including both HF and DFT. As these, then, often constitute the basis for more elaborate approaches such as (real-time) time-dependent *ansätze* as well as response-theory-based approaches and post-HF electron correlation approaches, in general, for example, configuration-interaction- or coupled-cluster-type wave function expansions, our (e)amfX2C models are broadly applicable within a two-component quantum-chemical framework.

As a first demonstration of the capabilities of the (e)amfX2C models, we have applied them to the calculation of molecular spinor energies of representative closed and open-shell (super)heavy homonuclear diatomic molecules of group 16 and 18, respectively, both within an HF and a DFT-based SCF *ansatz*. With these systems, viz., Te_2 and Og_2, we have assessed the numerical accuracy of the (e)amfX2C Hamiltonian models by comparing to four-component reference data with respect to the ability to reproduce absolute spinor energies as well as relative energies defined as the atomic-like spin–orbit splittings of the inner-core shells. As a further test, we have calculated both the absolute contact density at the Cn nucleus and contact density shifts in copernicium fluoride compounds (CnF_n, $n = 2, 4, 6$) relative to the atomic value for the bare Cn atom. Finally, we have studied the performance of our (e)amfX2C Hamiltonian models for core-electron binding energies in the realm of x-ray spectroscopy by making use of an equation-of-motion coupled-cluster approach.

For the open- and closed-shell diatomic molecules, we demonstrate that by applying our (e)amf PCE corrections to the X2C Hamiltonian models, it is possible to match all corresponding four-component molecular spinor energies with μ-Hartree accuracy, viz. for inner-core to outer-valence electronic shells. This outstanding performance holds not only for two-component SCF calculations within a Kramers-restricted and Kramers-unrestricted HF *ansatz* but also within a DFT framework. Moreover, we show that scalar-relativistic two-electron PCE corrections are of utmost importance for a reliable description of core electronic shells within a two-component X2C Hamiltonian framework. The latter necessity manifests itself also in the calculation of absolute as well as relative contact densities at the Cn nucleus with respect to CnF_n ($n = 0, 2, 4, 6$) compounds, where their neglect can lead to sizable discrepancies with respect to the same quantities obtained within a four-component framework. Although the (e)amf corrections are able to eliminate a substantial part of the scalar-relativistic and spin–orbit two-electron PCEs in the X2C framework, qualitative discrepancies between our two- and four-component results remain. We could trace the missing gap to the ^4DC reference data for the absolute contact density at the Cn nucleus in CnF_2 and, similarly, for the other CnF_n ($n > 2$) compounds, to a contact density contribution of the Cn 1s shell whose contributions show a relative deviation of about 11% between two- and four-component data.

Furthermore, in a comparison of x-ray core binding energies for At^-, $[AuCl_4]^{-1}$ and CnF_6 we highlighted the significance of an appropriate account of two-electron PCE corrections in a two-component framework that allows us to unambiguously and systematically approach reference $^4DC(G)$ results in the parent four-component framework. In particular, we demonstrate that our (e)amfX2C models enable X2C calculations of x-ray ionization potentials—and the accompanying resolution of fine-structure fingerprints of L- and M-edges in heavy- and superheavy-element complexes—where the transformation to two components is performed *prior* to the (molecular) SCF step while yielding results both on par with corresponding *molecular* mean-field calculations and in excellent agreement with the parent four-component ones. Moreover, we illustrate that it is possible within our (e)amfX2C models to account for two-electron effects originating from the Gaunt interaction. To ultimately strive for genuine comparisons of computed x-ray spectroscopic data with experiment, an inclusion of the full Breit interaction, higher-order correlation effects as well as QED corrections will be essential to establish a computational model of true predictive power.[89] While the former two factors are currently under consideration within the DIRAC developers' community,[108] QED corrections have very recently been put forward for correlated calculations in a two-component framework[109] and will be made available in a future extension of our (e)amfX2C models.

In summary, we are confident that the picture-change-error correction models for the X2C Hamiltonian presented in this contribution constitute an important milestone toward a universal and reliable applicability of relativistic two-component quantum-chemical approaches maintaining the accuracy of the parent four-component one at a fraction of its computational cost. In order to corroborate the latter, we are currently undertaking comprehensive studies of zero-field splittings in *p*- and *d*-block molecules as well as the calculations of EPR parameters of *d*- and *f*-element complexes on the basis of our (e)amfX2C Hamiltonian models within a correlated computational framework. Finally, since relativistic real-time time-dependent DFT[110] and wave function-based correlated approaches such as the density matrix renormalization group model[111] provide access to the absorption spectra of complex molecular systems in the valence- or core-excited range including a variational account of spin–orbit interaction, we intend to apply these approaches within our (e)amfX2C framework to a set of representative molecular *d*-block and actinide compounds.

DEDICATION

We dedicate this work to the memory of the late Bernd Schimmelpfennig, who passed away unexpectedly in 2019. He was, among other contributions, a pioneer in making corrections for two-electron picture-change effects within a two-component Hamiltonian framework not only popular but also, for the first time, widely usable in quantum chemistry.

ACKNOWLEDGMENTS

AUTHOR DECLARATIONS

Conflict of Interest

The authors have no conflicts to disclose.

Author Contributions

Stefan Knecht: Conceptualization (equal), Data curation (equal), Software (lead), Visualization (lead), Writing – original draft (equal), Writing – review & editing (equal), **Michal Repisky**: Conceptualization (equal), Software (equal), Validation (equal), Writing – original draft (equal), Writing – review & editing (equal), **Hans Jørgen Aagaard Jensen**: Conceptualization (equal), Writing – original draft (equal), Writing – review & editing (equal), **Trond Saue**: Conceptualization (equal), Writing – original draft (equal), Writing – review & editing (equal).

DATA AVAILABILITY

The data that support the findings of this study are openly available in ZENODO at https://doi.org/10.5281/zenodo.6414910, see also Ref. 112.

REFERENCES

[1] K. G. Dyall and K. Fægri, *Introduction to Relativistic Quantum Chemistry* (Oxford University Press, Oxford, 2007).

[2] M. Reiher and A. Wolf, *Relativistic Quantum Chemistry: The Fundamental Theory of Molecular Science* (Wiley VCH, Weinheim, 2009).

[3] T. Saue, "Relativistic Hamiltonians for chemistry: A primer," ChemPhysChem **12**, 3077–3094 (2011).

[4] W. Liu, "Advances in relativistic molecular quantum mechanics," Phys. Rep. **537**, 59–89 (2014).

[5] T. Saue, R. Bast, A. S. P. Gomes, H. J. Aa. Jensen, L. Visscher, I. A. Aucar, R. Di Remigio, K. G. Dyall, E. Eliav, E. Fasshauer, T. Fleig, L. Halbert, E. D. Hedegård, B. Helmich-Paris, M. Iliaš, C. R. Jacob, S. Knecht, J. K. Laerdahl, M. L. Vidal, M. K. Nayak, M. Olejniczak, J. M. H. Olsen, M. Pernpointner, B. Senjean, A. Shee, A. Sunaga, and J. N. P. van Stralen, "The DIRAC code for relativistic molecular calculations," J. Chem. Phys. **152**, 204104 (2020).

[6] M. Repisky, S. Komorovsky, M. Kadek, L. Konecny, U. Ekström, E. Malkin, M. Kaupp, K. Ruud, O. L. Malkina, and V. G. Malkin, "ReSpect: Relativistic spectroscopy DFT program package," J. Chem. Phys. **152**, 184101 (2020).

[7] T. Shiozaki, "BAGEL: Brilliantly advanced general electronic-structure library," WIREs comput. Mol. Sci. **8**, e1331 (2018).

[8] Y. Zhang, B. Suo, Z. Wang, N. Zhang, Z. Li, Y. Lei, W. Zou, J. Gao, D. Peng, Z. Pu, Y. Xiao, Q. Sun, F. Wang, Y. Ma, X. Wang, Y. Guo, and W. Liu, "BDF: A relativistic electronic structure program package," J. Chem. Phys. **152**, 064113 (2020).

[9] L. Belpassi, M. De Santis, H. M. Quiney, F. Tarantelli, and L. Storchi, "BERTHA: Implementation of a four-component Dirac–Kohn–Sham relativistic framework," J. Chem. Phys. **152**, 164118 (2020).

[10] The generic acronym "X2C" for exact two-component Hamiltonians resulted from intensive discussions among H. J. Aa. Jensen, W. Kutzelnigg, W. Liu, T. Saue,

and L. Visscher during the Twelfth International Conference on the Applications of Density Functional Theory DFT-2007, Amsterdam, 26–30 August 2007.

[11] M. Douglas and N. M. Kroll, "Quantum electrodynamical corrections to the fine structure of helium," Ann. Phys. **82**, 89–155 (1974).

[12] B. A. Hess, "Relativistic electronic-structure calculations employing a two-component No-pair formalism with external-field projection operators," Phys. Rev. A **33**, 3742–3748 (1986).

[13] C. Chang, M. Pelissier, and P. Durand, "Regular two-component Pauli-like effective Hamiltonians in Dirac theory," Phys. Scr. **34**, 394 (1986).

[14] E. v. Lenthe, E. J. Baerends, and J. G. Snijders, "Relativistic regular two-component Hamiltonians," J. Chem. Phys. **99**, 4597 (1993).

[15] E. van Lenthe, J. G. Snijders, and E. J. Baerends, "The zero-order regular approximation for relativistic effects: The effect of spin–orbit coupling in closed shell molecules," J. Chem. Phys. **105**, 6505 (1996).

[16] M. Barysz and A. J. Sadlej, "Infinite-order two-component theory for relativistic quantum chemistry," J. Chem. Phys. **116**, 2696 (2002).

[17] M. Reiher and A. Wolf, "Exact decoupling of the Dirac Hamiltonian. I. General theory," J. Chem. Phys. **121**, 2037 (2004).

[18] M. Reiher and A. Wolf, "Exact decoupling of the Dirac Hamiltonian. II. The generalized Douglas–Kroll–Hess transformation up to arbitrary order," J. Chem. Phys. **121**, 10945 (2004).

[19] M. Reiher, "Douglas–Kroll–Hess theory: A relativistic electrons-only theory for chemistry," Theor. Chem. Acc. **116**, 241–252 (2006).

[20] K. G. Dyall, "Interfacing relativistic and nonrelativistic methods. I. Normalized elimination of the small component in the modified Dirac equation," J. Chem. Phys. **106**, 9618 (1997).

[21] M. Filatov and D. Cremer, "Connection between the regular approximation and the normalized elimination of the small component in relativistic quantum theory," J. Chem. Phys. **122**, 064104 (2004).

[22] M. Filatov, "Comment on 'Quasirelativistic theory equivalent to fully relativistic theory' [J.Chem. Phys. 123, 241102 (2005)]," J. Chem. Phys. **125**, 107101 (2006).

[23] M. Filatov and K. G. Dyall, "On convergence of the normalized elimination of the small component (NESC) method," Theor. Chem. Acc. **117**, 333–338 (2007).

[24] H. J. Aa. Jensen and M. Iliaš, BSS/DKH infinite order the easy way!, https://doi.org/10.6084/m9.figshare.12046158.v3 (2005), (Talk from REHE 2005).

[25] W. Kutzelnigg and W. Liu, "Quasirelativistic theory equivalent to fully relativistic theory," J. Chem. Phys. **123**, 241102 (2005).

[26] W. Kutzelnigg and W. Liu*, "Quasirelativistic theory I. Theory in terms of a quasi-relativistic operator," Mol. Phys. **104**, 2225 (2006).

[27] W. Liu and D. Peng, "Infinite-order quasirelativistic density functional method based on the exact matrix quasirelativistic theory," J. Chem. Phys. **125**, 044102 (2006).

[28] M. Iliaš and T. Saue, "An infinite-order two-component relativistic Hamiltonian by a simple one-step transformation," J. Chem. Phys. **126**, 064102 (2007).

[29] W. Liu and D. Peng, "Exact two-component Hamiltonians revisited," J. Chem. Phys. **131**, 031104 (2009).

[30] L. Konecny, M. Kadek, S. Komorovsky, O. L. Malkina, K. Ruud, and M. Repisky, "Acceleration of relativistic electron dynamics by means of X2C transformation: Application to the calculation of nonlinear optical properties," J. Chem. Theory Comput. **12**, 5823–5833 (2016).

[31] D. Peng and M. Reiher, "Exact decoupling of the relativistic Fock operator," Theor. Chem. Acc. **131**, 1081–1100 (2012).

[32] J. Sikkema, L. Visscher, T. Saue, and M. Iliaš, "The molecular mean-field approach for correlated relativistic calculations," J. Chem. Phys. **131**, 124116 (2009).

[33] K. G. Dyall, "An exact separation of the spin-free and spin-dependent terms of the Dirac–Coulomb–Breit Hamiltonian," J. Chem. Phys. **100**, 2118 (1994).

[34] J. Liu and L. Cheng, "An atomic mean-field spin-orbit approach within exact two-component theory for a non-perturbative treatment of spin-orbit coupling," J. Chem. Phys. **148**, 144108 (2018).

[35] M. Blume and R. E. Watson, "Theory of spin-orbit coupling in atoms I. Derivation of the spin-orbit coupling constant," Proc. R. Soc. Lond. A **270**, 127–143 (1962).

[36].M. Blume and R. E. Watson, "Theory of spin-orbit coupling in atoms, II. Comparison of theory with experiment," Proc. R. Soc. Lond. A **271**, 565–578 (1963).

[37]B. A. Heß, C. M. Marian, U. Wahlgren, and O. Gropen, "A mean-field spin-orbit method applicable to correlated wavefunctions," Chem. Phys. Lett. **251**, 365 (1996).

[38]AMFI, an atomic mean-field spin-orbit integral program, 1996, Bernd Schimmelpfennig, University of Stockholm.

[39]I. Fdez. Galván, M. Vacher, A. Alavi, C. Angeli, F. Aquilante, J. Autschbach, J. J. Bao, S. I. Bokarev, N. A. Bogdanov, R. K. Carlson, L. F. Chibotaru, J. Creutzberg, N. Dattani, M. G. Delcey, S. S. Dong, A. Dreuw, L. Freitag, L. M. Frutos, L. Gagliardi, F. Gendron, A. Giussani, L. González, G. Grell, M. Guo, C. E. Hoyer, M. Johansson, S. Keller, S. Knecht, G. Kovačević, E. Källman, G. Li Manni, M. Lundberg, Y. Ma, S. Mai, J. P. Malhado, P. Å. Malmqvist, P. Marquetand, S. A. Mewes, J. Norell, M. Olivucci, M. Oppel, Q. M. Phung, K. Pierloot, F. Plasser, M. Reiher, A. M. Sand, I. Schapiro, P. Sharma, C. J. Stein, L. K. Sørensen, D. G. Truhlar, M. Ugandi, L. Ungur, A. Valentini, S. Vancoillie, V. Veryazov, O. Weser, T. A. Wesołowski, P.-O. Widmark, S. Wouters, A. Zech, J. P. Zobel, and R. Lindh, "OpenMolcas: From source code to insight," J. Chem. Theory Comput. **15**, 5925–5964 (2019).

[40]K. Aidas, C. Angeli, K. L. Bak, V. Bakken, R. Bast, L. Boman, O. Christiansen, R. Cimiraglia, S. Coriani, P. Dahle, E. K. Dalskov, U. Ekström, T. Enevoldsen, J. J. Eriksen, P. Ettenhuber, B. Fernández, L. Ferrighi, H. Fliegl, L. Frediani, K. Hald, A. Halkier, C. Hättig, H. Heiberg, T. Helgaker, A. C. Hennum, H. Hettema, E. Hjertenaes, S. Høst, I.-M. Høyvik, M. F. Iozzi, B. Jansík, H. J. Aa. Jensen, D. Jonsson, P. Jørgensen, J. Kauczor, S. Kirpekar, T. Kjaergaard, W. Klopper, S. Knecht, R. Kobayashi, H. Koch, J. Kongsted, A. Krapp, K. Kristensen, A. Ligabue, O. B. Lutnaes, J. I. Melo, K. V. Mikkelsen, R. H. Myhre, C. Neiss, C. B. Nielsen, P. Norman, J. Olsen, J. M. H. Olsen, A. Osted, M. J. Packer, F. Pawlowski, T. B. Pedersen, P. F. Provasi, S. Reine, Z. Rinkevicius, T. A. Ruden, K. Ruud, V. V. Rybkin, P. Sałek, C. C. M. Samson, A. S. de Merás, T. Saue, S. P. A. Sauer, B. Schimmelpfennig, K. Sneskov, A. H. Steindal, K. O. Sylvester-Hvid, P. R. Taylor, A. M. Teale, E. I. Tellgren, D. P. Tew, A. J. Thorvaldsen, L. Thøgersen, O. Vahtras, M. A. Watson, D. J. D. Wilson, M. Ziolkowski, and H. Ågren, "The Dalton quantum chemistry program system," WIREs Comput. Mol. Sci. **4**, 269–284 (2014).

[41]C. van Wüllen and C. Michauk, "Accurate and efficient treatment of two-electron contributions in quasirelativistic high-order Douglas-Kroll density-functional calculations," J. Chem. Phys. **123**, 204113 (2005).

[42]D. Peng, W. Liu, Y. Xiao, and L. Cheng, "Making four- and two-component relativistic density functional methods fully equivalent based on the idea of "from atoms to molecule","" J. Chem. Phys. **127**, 104106 (2007).

[43]J. Autschbach, D. Peng, and M. Reiher, "Two-component relativistic calculations of electric-field gradients using exact decoupling methods: Spin-orbit and picture-change effects," J. Chem. Theory Comput. **8**, 4239–4248 (2012).

[44]J. C. Boettger, "Approximate two-electron spin-orbit coupling term for density-functional-theory DFT calculations using the Douglas–Kroll–Hess transformation," Phys. Rev. B **62**, 7809–7815 (2000).

[45]A. J. Jenkins, H. Liu, J. M. Kasper, M. J. Frisch, and X. Li, "Variational relativistic Two-Component complete-active-space self-consistent field method," J. Chem. Theory Comput. **15**, 2974–2982 (2019).

[46]L. N. Koulias, D. B. Williams-Young, D. R. Nascimento, A. E. DePrince, and X. Li, "Relativistic real-time time-dependent equation-of-motion coupled-cluster," J. Chem. Theory Comput. **15**, 6617–6624 (2019).

[47]H. Hu, A. J. Jenkins, H. Liu, J. M. Kasper, M. J. Frisch, and X. Li, "Relativistic two-component multireference configuration interaction method with tunable correlation space," J. Chem. Theory Comput. **16**, 2975–2984 (2020).

[48]M. Filatov, W. Zou, and D. Cremer, "Spin-orbit coupling calculations with the two-component normalized elimination of the small component method," J. Chem. Phys. **139**, 014106 (2013).

[49]W. Zou, M. Filatov, and D. Cremer, "Analytical energy gradient for the two-component normalized elimination of the small component method," J. Chem. Phys. **142**, 214106 (2015).

[50]J. Liu and L. Cheng, "Relativistic coupled-cluster and equation-of-motion coupled-cluster methods," WIREs Comput Mol. Sci. **11**, e1536 (2021).

[51]J. Netz, A. O. Mitrushchenkov, and A. Köhn, "On the accuracy of mean-field spin–orbit operators for 3d transition-metal systems," J. Chem. Theory Comput. **17**, 5530 (2021).

[52]P.-O. Löwdin, "On the nonorthogonality problem," Adv.Quant.Chem. **5**, 185 (1970).

[53]J. Thyssen, "Development and applications of methods for correlated relativistic calculations of molecular properties," Ph.D. thesis, University of Southern Denmark, 2001.

[54]J. P. Perdew, R. G. Parr, M. Levy, and J. L. Balduz, "Density-functional theory for fractional particle number: Derivative discontinuities of the energy," Phys. Rev. Lett. **49**, 1691–1694 (1982).

[55]J. P. Perdew and K. Schmidt, in *Density Functional Theory and its Application to Materials*, edited by V. V. Doren, C. V. Alsenoy, and P. Geerlings (American Institute of Physics, Melville, 2001).

[56]J. P. Perdew, A. Ruzsinszky, J. Tao, V. N. Staroverov, G. E. Scuseria, and G. I. Csonka, "Prescription for the design and selection of density functional approximations: More constraint satisfaction with fewer fits," J. Chem. Phys. **123**, 062201 (2005).

[57]Y. Ikabata and H. Nakai, "Picture-change correction in relativistic density functional theory," Phys. Chem. Chem. Phys. **23**, 15458–15474 (2021).

[58]S. Komorovsky, P. J. Cherry, and M. Repisky, "Four-component relativistic time-dependent density-functional theory using a stable noncollinear DFT ansatz applicable to both closed- and open-shell systems," J. Chem. Phys. **151**, 184111 (2019).

[59]J. Kubler, K.-H. Hock, J. Sticht, and A. R. Williams, "Density functional theory of non-collinear magnetism," J. Phys. F: Met. Phys. **18**, 469–483 (1988).

[60]L. M. Sandratskii, "Noncollinear magnetism in itinerant-electron systems: Theory and applications," Adv. Phys. **47**, 91–160 (1998).

[61]C. van Wüllen, "Spin densities in two-component relativistic density functional calculations: Noncollinear versus collinear approach," J. Comp. Chem. **23**, 779–785 (2002).

[62]G. Scalmani and M. J. Frisch, "A new approach to noncollinear spin density functional theory beyond the local density approximation," J. Chem. Theory Comput. **8**, 2193–2196 (2012).

[63]J. H. van Lenthe, R. Zwaans, J. J. H. van Dam, and M. F. Guest, "Starting SCF calculations by superposition of atomic densities," J. Comp. Chem. **27**, 926–932 (2006).

[64]P. J. Mohr, B. N. Taylor, and D. B. Newell, "CODATA recommended values of the fundamental physical constants: 2006," Rev. Mod. Phys. **80**, 633–730 (2008).

[65]K. G. Dyall, "Relativistic double-zeta, triple-zeta, and quadruple-zeta basis sets for the light elements H–Ar," Theor. Chem. Acc. **135**, 128 (2016).

[66]K. G. Dyall, "Relativistic and nonrelativistic finite nucleus optimized double zeta basis sets for the 4p, 5p and 6p elements," Theor. Chem. Acc. **99**, 366–371 (1998).

[67]K. G. Dyall, "Relativistic quadruple-zeta and revised triple-zeta and double-zeta basis sets for the 4p, 5p, and 6p elements," Theor. Chem. Acc. **115**, 441–447 (2006).

[68]K. G. Dyall, "Relativistic double-zeta, triple-zeta, and quadruple-zeta basis sets for the 7p elements, with atomic and molecular applications," Theor. Chem. Acc. **131**, 1172 (2012).

[69]K. G. Dyall, "Relativistic double-zeta, triple-zeta, and quadruple-zeta basis sets for the 5d elements Hf–Hg," Theor. Chem. Acc. **112**, 403–409 (2004).

[70]K. G. Dyall and A. S. P. Gomes, "Revised relativistic basis sets for the 5d elements Hf–Hg," Theor. Chem. Acc. **125**, 97–100 (2009).

[71]K. G. Dyall, "Relativistic double-zeta, triple-zeta, and quadruple-zeta basis sets for the 6d elements Rf–Cn," Theor. Chem. Acc. **129**, 603–613 (2011).

[72]Available from the Dirac web site, http://dirac.chem.sdu.dk.

[73]R. Lindh, P. Å. Malmqvist, and L. Gagliardi, "Molecular integrals by numerical quadrature. I. Radial integration," Theor. Chem. Acc. **106**, 178–187 (2001).

[74]V. Lebedev, "Values of the nodes and weights of ninth to seventeenth order gauss-markov quadrature formulae invariant under the octahedron group with inversion," Zh. Vychisl. Mat. Mat. Fiz. **15**, 48–54 (1975).

[75]V. Lebedev, "Quadratures on a sphere," Zh. Vychisl. Mat. Mat. Fiz. **16**, 293–306 (1976).

[76]V. I. Lebedev, "Spherical quadrature formulas exact to orders 25–29," Sibirsk. Mat. Zh. **18**, 132–142 (1977).

[77]P. Pulay, "Convergence acceleration of iterative sequences. The case of SCF iteration," Chemical Physics Letters **73**, 393–398 (1980).

[78]J. P. Perdew, K. Burke, and M. Ernzerhof, "Generalized gradient approximation made simple," Phys. Rev. Lett. **77**, 3865–3868 (1996).

[79] J. P. Perdew, M. Ernzerhof, and K. Burke, "Rationale for mixing exact exchange with density functional approximations," J. Chem. Phys. **105**, 9982–9985 (1996).

[80] C. Adamo and V. Barone, "Toward chemical accuracy in the computation of NMR shieldings: The PBE0 model," Chem. Phys. Lett. **298**, 113–119 (1998).

[81] J. F. Ogilvie and F. Y. H. Wang, "Potential-energy functions of diatomic molecules of the noble gases I. Like nuclear species," J. Mol. Struct. **273**, 277–290 (1992).

[82] A. Shee, S. Knecht, and T. Saue, "A theoretical benchmark study of the spectroscopic constants of the very heavy rare gas dimers," Phys. Chem. Chem. Phys. **17**, 10978 (2015).

[83] J.-B. Rota, S. Knecht, T. Fleig, D. Ganyushin, T. Saue, F. Neese, and H. Bolvin, "Zero field splitting of the chalcogen diatomics using relativistic correlated wave-function methods," J. Chem. Phys. **135**, 114106 (2011).

[84] L. Trombach, S. Ehlert, S. Grimme, P. Schwerdtfeger, and J.-M. Mewes, "Exploring the chemical nature of super-heavy main-group elements by means of efficient plane-wave density-functional theory," Phys. Chem. Chem. Phys. **21**, 18048–18058 (2019).

[85] S.-X. Hu and W. Zou, "Stable copernicium hexafluoride (CnF_6) with an oxidation state of VI+," Phys. Chem. Chem. Phys. **24**, 321 (2022).

[86] S. Knecht, S. Fux, R. van Meer, L. Visscher, M. Reiher, and T. Saue, "Mössbauer spectroscopy for heavy elements: A relativistic benchmark study of mercury," Theor. Chem. Acc. **129**, 631–650 (2011).

[87] S. Knecht and T. Saue, "Nuclear size effects in rotational spectra: A tale with a twist," Chem. Phys. **401**, 103–112 (2012).

[88] A. Shee, T. Saue, L. Visscher, and A. Severo Pereira Gomes, "Equation-of-Motion coupled-cluster theory based on the 4-component Dirac–Coulomb(–Gaunt) Hamiltonian. Energies for single electron detachment, attachment, and electronically excited states," J. Chem. Phys. **149**, 174113 (2018).

[89] L. Halbert, M. L. Vidal, A. Shee, S. Coriani, and A. Severo Pereira Gomes, "Relativistic EOM-CCSD for core-excited and core-ionized state energies based on the four-component Dirac–Coulomb(-Gaunt) Hamiltonian," J. Chem. Theory Comput. **17**, 3583–3598 (2021).

[90] M. Hargittai, A. Schulz, B. Réffy, and M. Kolonits, "Molecular structure, bonding, and Jahn–Teller effect in gold chlorides: Quantum chemical study of $AuCl_3$, Au_2Cl_6, $AuCl_4^-$, $AuCl$, and Au_2Cl_2 and electron diffraction study of Au_2Cl_6," J. Am. Chem. Soc. **123**, 1449–1458 (2001).

[91] M. A. Ambroise, A. Dreuw, and F. Jensen, "Probing basis set requirements for calculating core ionization and core excitation spectra using correlated wave function methods," J. Chem. Theory Comput. **17**, 2832–2842 (2021).

[92] L. Visscher and T. Saue, "Approximate relativistic electronic structure methods based on the quaternion modified Dirac equation," J. Chem. Phys. **113**, 3996–4002 (2000).

[93] T. Saue, "Principles and applications of relativistic molecular calculations," Ph.D. thesis, University of Oslo, 1996.

[94] C. Pellegrini, A. Marinelli, and S. Reiche, "The physics of X-ray free-electron lasers," Rev. Mod. Phys. **88**, 015006 (2016).

[95] See https://www.xfel.eu/facility/comparison/index_eng.html for An overview on X-ray free-electron laser facilities.

[96] F. Lin, Y. Liu, X. Yu, L. Cheng, A. Singer, O. G. Shpyrko, H. L. Xin, N. Tamura, C. Tian, T.-C. Weng, X.-Q. Yang, Y. S. Meng, D. Nordlund, W. Yang, and M. M. Doeff, "Synchrotron X-ray analytical techniques for studying materials electrochemistry in rechargeable batteries," Chem. Rev. **117**, 13123–13186 (2017).

[97] M. Chergui and E. Collet, "Photoinduced structural dynamics of molecular systems mapped by time-resolved X-ray methods," Chem. Rev. **117**, 11025–11065 (2017).

[98] P. M. Kraus, M. Zürch, S. K. Cushing, D. M. Neumark, and S. R. Leone, "The ultrafast X-ray spectroscopic revolution in chemical dynamics," Nat. Rev. Chem. **2**, 82–94 (2018).

[99] P. Norman and A. Dreuw, "Simulating X-ray spectroscopies and calculating core-excited states of molecules," Chem. Rev. **118**, 7208–7248 (2018).

[100] K. O. Kvashnina and S. M. Butorin, "High-energy resolution X-ray spectroscopy at actinide $M_{4,5}$ and ligand K edges: What we know, what we want to know, and what we can know," Chem. Commun. **58**, 327–342 (2022).

[101] M. Kadek, L. Konecny, B. Gao, M. Repisky, and K. Ruud, "X-Ray absorption resonances near $L_{2,3}$-edges from real-time propagation of the Dirac–Kohn–Sham density matrix," Phys. Chem. Chem. Phys. **17**, 22566–22570 (2015).

[102] C. South, A. Shee, D. Mukherjee, A. K. Wilson, and T. Saue, "4-Component relativistic calculations of L3 ionization and excitations for the isoelectronic species UO_2^{2+} OUN^+ and UN_2," Phys. Chem. Chem. Phys. **18**, 21010 (2016).

[103] T. F. Stetina, J. M. Kasper, and X. Li, "Modeling $L_{2,3}$-edge X-ray absorption spectroscopy with linear response exact two-component relativistic time-dependent density functional theory," J. Chem. Phys. **150**, 234103 (2019).

[104] L. Konecny, J. Vicha, S. Komorovsky, K. Ruud, and M. Repisky, "Accurate X-ray absorption spectra near L- and M-edges from relativistic four-component damped response time-dependent density functional theory," Inorg. Chem. **61**, 830–846 (2022).

[105] C. Puzzarini, J. Bloino, N. Tasinato, and V. Barone, "Accuracy and interpretability: The devil and the holy grail. New routes across old boundaries in computational spectroscopy," Chem. Rev. **119**, 8131–8191 (2019).

[106] The scalar relativistic atomic SCF code relscf is based on an atomic SCF code written by Enrico Clementi [*Ab initio computations in atoms and molecules*, IBM Journal Res. and Develop. **9**, 2–19, (1965)] and scalar relativity was introduced by Bernd Hess.

[107] M. Kadek, M. Repisky, and K. Ruud, "All-electron fully relativistic Kohn-Sham theory for solids based on the Dirac-Coulomb Hamiltonian and Gaussian-type functions," Phys. Rev. B **99**, 205103 (2019).

[108] Private communications, DIRAC developers meeting 2021, online, Sep 2nd (2021).

[109] A. Sunaga and T. Saue, "Towards highly accurate calculations of parity violation in chiral molecules: Relativistic coupled-cluster theory including QED-effects," Mol. Phys. **119**, e1974592 (2021).

[110] M. Repisky, L. Konecny, M. Kadek, S. Komorovsky, O. L. Malkin, V. G. Malkin, and K. Ruud, "Excitation energies from real-time propagation of the four-component Dirac-Kohn-Sham equation," J. Chem. Theory Comput. **11**, 980–991 (2015).

[111] B. Alberto, private communication (March 2022).

[112] S. Knecht, M. Repisky, H. J. Aa. Jensen, and T. Saue (2022), "Replication data for: Exact two-component Hamiltonians for relativistic quantum chemistry: Two-electron picture-change corrections made simple," Zenodo. https://doi.org/10.5281/zenodo.6414910